Potential contributions of nitrifiers and denitrifiers to nitrous oxide sources and sinks in China's estuarine and coastal areas

Xiaofeng Dai[1], Mingming Chen[1], Xianhui Wan[2], Ehui Tan[3], Jialing Zeng[1], Nengwang Chen[1, 4], Shuh-Ji Kao[1, 3], Yao Zhang[1*]

[1]State Key Laboratory of Marine Environmental Science, College of Ocean and Earth Sciences, Xiamen University, Xiamen 361005, China

[2]Department of Geosciences, Princeton University, NJ 08540, USA.

[3]State Key Laboratory of Marine Resource Utilization in South China Sea, Hainan University, Haikou, Hainan, China

[4]Fujian Provincial Key Laboratory for Coastal Ecology and Environmental Studies, College of the Environment and Ecology, Xiamen University, Xiamen 361005, China

Correspondence to: Yao Zhang (yaozhang@xmu.edu.cn)

Abstract. Nitrous oxide (N_2O) is an important ozone-depleting greenhouse gas produced and consumed by microbially mediated nitrification and denitrification pathways. Estuaries are intensive N_2O emission regions in marine ecosystems. However, the potential contributions of nitrifiers and denitrifiers to N_2O sources and sinks in China's estuarine and coastal areas are poorly understood. The abundance and transcription of six key microbial functional genes involved in nitrification and denitrification, as well as the clade II-type *nosZ* gene-bearing community composition of N_2O reducers, were investigated in four estuaries spanning the Chinese coastline. The results showed that the ammonia-oxidizing archaeal *amoA* genes and transcripts were more dominant in the northern Bohai Sea (BS) and Yangtze River estuaries, which had low nitrogen concentrations, while the denitrifier *nirS* genes and transcripts were more dominant in the southern Jiulong River (JRE) and Pearl River estuaries, which had high levels of terrestrial nitrogen input. Notably, the *nosZ* clade II gene was more abundant than the clade I-type throughout the estuaries except for in the JRE and a few sites of the BS, while the opposite transcript distribution pattern was observed in these two estuaries. The gene and transcript distributions were significantly constrained by nitrogen and oxygen concentrations, as well as salinity, temperature, and pH. The *nosZ* clade II gene-bearing community composition along China's coastline had a high diversity and was distinctly different from that in the soil and marine oxygen-minimum-zone waters. By comparing

the gene distribution patterns across the estuaries with the distribution patterns of the N$_2$O concentration and flux, we found that denitrification may principally control the N$_2$O emissions pattern.

1 Introduction

Nitrous oxide (N$_2$O) is a kind of ozone-depleting substance and an important, long-lived greenhouse gas with 298 times the single mole global warming potential of carbon dioxide (CO$_2$) (IPCC 2007; Ravishankara et al., 2009; Rowley et al., 2013). Prokaryotic microorganisms play an important role in N$_2$O production and consumption through the nitrification and denitrification pathways (Babbin et al., 2015; Domeignoz-Horta1 et al., 2015; Ji et al., 2018b; Meinhardt et al., 2018; Santoro et al., 2011; Silvennoinen et al., 2008). N$_2$O is produced as a byproduct in the first step (NH$_4^+$→NO$_2^-$) of nitrification, which is catalyzed by ammonia monooxygenase in ammonia-oxidizing archaea (AOA) and ammonia-oxidizing bacteria (AOB) (Codispoti and Christensen, 1985). The ammonia monooxygenase subunit A gene (*amoA*) is frequently used as a functional gene marker for AOA and AOB analysis. N$_2$O is also produced as a kind of intermediate product in the denitrification process, in which nitrite (NO$_2^-$) is reduced to nitric oxide (NO) and then further reduced to N$_2$O. Usually, the nitrite reductase genes *nirS* and *nirK* are used to evaluate the N$_2$O production potential through denitrification (Hallin et al., 2018; Shaw et al., 2006; Wrage et al., 2001). Some bacterial nitrifiers can also reduce NO$_2^-$ to N$_2$O through a nitrifier denitrification pathway. The last step of denitrification is the only known biological N$_2$O consumption pathway, reducing N$_2$O into nitrogen (N$_2$) under the catalysis of nitrous oxide reductase encoded by the *nosZ* gene. This gene is divided into two clades according to the differences in the signal peptides of nitrous oxide reductase (Henry et al., 2006; Jones et al., 2013). The microorganisms possessing clade I-type *nosZ* genes are mainly affiliated with alpha-, beta-, and gamma-proteobacteria, and the clade I gene has a higher frequency of co-occurrence with *nir* and *nor* genes than the clade II gene. The *nosZ* clade II genes are present in a much larger range of archaeal and bacterial phyla (Jones et al., 2013), and intergenomic comparisons have revealed that more than half of the microorganisms possessing clade II genes lack nitrite reductase or nitric oxide reductase, do not produce N$_2$O, and thus are expected to drive potential N$_2$O sinks (Graf et al., 2014; Jones et al., 2008; Marchant et al., 2017; Sanford et al., 2012). The community composition of microorganisms with *nosZ* clade II genes is considered important for the N$_2$O:N$_2$ end-product ratio of denitrification, influencing the regional N$_2$O

source or sink characteristics (Domeignoz-Horta1 et al., 2015; Philippot, 2013). However, there are few studies on *nosZ* clade II gene diversity and community composition in Chinese estuarine and coastal areas.

Decades of research have revealed that the ocean is the second most important source of N_2O emissions following arable soils, contributing one-third of the N_2O emission fluxes to the atmosphere (Nevison et al., 2003). Estuaries, as important bioreactors, are the most active N_2O exchange areas in the ocean, accounting for 33% of oceanic N_2O emissions with only approximately 0.4% of the area (Bange et al., 1996; Zhang et al., 2010). Denitrification is the major contributor to N_2O production in terrestrial ecosystems and stream and river networks (Beaulieu et al., 2011; Marzadri et al., 2017). However, complete denitrification can consume N_2O (Jones et al., 2014). A recent study reports a fourfold increase in global riverine N_2O emissions influenced by human activities (Yao et al., 2020). Marine nitrification supported by ammonia-oxidizing archaea is largely responsible for oceanic N_2O emissions, especially in the open ocean (Löscher et al., 2012; Santoro et al., 2011), while nitrate reduction is the dominant N_2O source in oxygen minimum zones (OMZs) (Frey et al., 2020; Ji et al., 2018a; Yamagishi et al., 2007). In estuaries, the transition zones between the land and sea, both nitrification and denitrification could be dominant driving processes of active N_2O exchange. For example, nitrification was credited as the dominant N_2O production pathway in the Schelde Estuary as well as in some other European estuaries (Barnes and Upstill-Goddard, 2011; Brase et al., 2017; De Wilde and De Bie, 2000), while an inverse correlation between N_2O concentration and oxygen indicates that denitrifiers might be the dominant N_2O contributor in the Potomac River estuary (McElroy et al., 1978). In addition, the incubation experiments with nitrogen stable isotope tracer reveal active N_2O production by denitrification in the Chesapeake Bay (Ji et al., 2018b). Another research in the Chesapeake Bay reveals that physical processes such as wind events and vertical mixing affect the net balance between N_2O production and consumption, resulting in a variable source and sink for N_2O (Laperriere et al., 2019).

The four main estuaries along the Chinese coastline include the Bohai Sea (BS) in the north, the Yangtze River Estuary (YRE) and the adjacent East China Sea (ECS) in the middle, as well as the Jiulong River Estuary (JRE) and Pearl River Estuary (PRE) in the south (Fig. 1). The BS is a semi-enclosed sea located in the north temperate zone of China. Influenced by frequent human activities and seasonal

variability in inputs from the Yellow River, Liao River, Luan River, and Hai River, seasonal hypoxia is an important characteristic of the BS (Chen, 2009). The YRE and the adjacent ECS, which receive a large amount of nutrients from the largest river in Asia (Yangtze River: runoff 9.2×10^{11} m^3 yr^{-1}) (Zhang, 2002), also exhibit seasonal hypoxia off the estuary from July to September because of the enhanced primary productivity (Zhu et al., 2011). Both the JRE and PRE are located in densely populated and industrialized subtropical areas, with runoffs of 1.44×10^{10} m^3 yr^{-1} and 3.26×10^{11} m^3 yr^{-1}, respectively (Cao et al., 2005; He et al., 2014). To clarify the potential contributions of nitrification and denitrification to sources and sinks of N_2O in China's estuarine and coastal aeras, the abundance and transcription activity of six key microbial functional genes involved in nitrification and denitrification (AOA and AOB *amoA*, *nirS*, *nirK*, *nosZ* clade I and II genes) were investigated in the four estuarine areas. In addition, the *nosZ* clade II gene diversity and N_2O reducing community composition were analyzed based on clone libraries to assess the local N_2O sink potential.

2 Materials and methods

2.1 Sampling and biogeochemical parameter measurements

A total of 228 (130 for DNA and 98 for RNA) samples from fifty-four sites were collected (Fig. 1). One hundred and sixteen samples (58 for DNA and for 58 for RNA) were collected from 20 stations with two or three depth layers (3–63 m; Table S1) in the BS on the R/V Dongfanghong #2 from August to September 2018. Seventy-four (41 for DNA and 33 for RNA) samples were collected from 16 stations with one to four depth layers (3–55 m) in the YRE on the R/V Yanping II from July to August 2017. Water samples were collected using a rosette sampler fitted with Niskin bottles (SBE 911, Sea-Bird Co). Sixteen surface samples (9 for DNA and 7 for RNA) from a water depth of ~0.5 m were collected from the JRE on the R/V Ocean II during September 2016. Twenty-two samples for DNA were collected from 11 stations with two depth layers (0.5–18 m) in the PRE on the R/V Wanyu during January 2017. Water samples were collected using an organic glass hydrophore (1 L; Kedun Co., China). In addition, 2 and 1 surface sediment samples were acquired using a grab sampler from the JRE in December 2015 and from the YRE from July to August 2017, respectively. Water samples of 0.2–2.5 L were filtered through 0.22 μm pore size polycarbonate membranes (Millipore, USA) within 1 h at a <0.03 MPa pressure for quantitative PCR (qPCR) analysis. Water samples were serially filtered through 10, 3, and 0.22 μm pore

size polycarbonate membranes (Millipore, USA) for clone library analysis (Table S1). The membranes

for RNA extraction were immediately fixed with 1.5 mL of RNAlater (Invitrogen, Life Technologies).

120   All filters and sediment samples were quick-frozen in liquid nitrogen and then stored at –80 °C for

laboratory analysis.

Temperature, salinity, and depth were measured using conductivity temperature depth (CTD) (SBE

911, Sea-Bird Co.) in the BS, YRE, and PRE. In the JRE, water temperature and salinity were

continuously measured (every 3 s for 1 min) using a YSI6600D salinometer installed on an underway

125   pumping system (Yan et al., 2019). Dissolved oxygen (DO) concentrations were measured using a WTW

multiparameter portable meter (Multi 3430, Germany). Ammonia was analyzed on deck using the

indophenol blue spectrophotometric method. Nitrate, nitrite, and silicate were measured using an AA3

Autoanalyzer (Bran+Luebbe Co., Germany) (Dai et al., 2008).

130   **2.2 Nucleic acid extraction, clone library, and phylogenetic analysis**

DNA from water samples was extracted using the phenol-chloroform-isoamyl alcohol method (Massana

et al., 1997) with minor modifications to maximize the DNA output. Briefly, tubes containing shredded

filters, approximately 0.5 g of 0.1 mm glass beads, and 800 µL of STE lysis buffer (0.75 M sucrose, 50

mM Tris-HCl, 40 mM EDTA) were first agitated for 60 s on a FastPrep machine (MP Biomedicals,

135   Solon, OH, USA) at 4.5 m s^{-1}. Then, the mixture was processed with lysozyme (1 mg ml^{-1}), proteinase

K (0.5 mg ml^{-1}), and sodium dodecyl sulfate (SDS) (1%) sequentially. At last, the lysate was extracted

twice with phenol-chloroform-isoamyl alcohol and once with chloroform-isoamyl alcohol. DNA was

precipitated with isopropyl alcohol and washed with 75% ethyl alcohol before dissolved in 50 µL sterile

water. DNA from sediment samples was extracted using a FastDNA SPIN Kit for Soil (MP Biomedicals,

140   USA). RNA from water samples was extracted using the RNeasy Mini kit according to the manual

(Qiagen, USA). Clean RNA, which was verified by the amplification of the bacterial 16S rRNA gene

with the primer set 342F/798R, was reverse transcribed to cDNA by the SuperScript III first strand

synthesis system (Invitrogen, Life Technologies) using random hexamers following the user manual. The

quality of both the DNA and cDNA was checked by amplifying the full-length bacterial 16S rRNA gene

145   before storage at –80 °C.

A total of 19 DNA samples (16 from water and 3 from sediment) from the four estuaries (Figs. 1 and 4) were used to construct clone libraries for the clade II-type *nosZ* gene. PCR was run with the primer set nosZ-II-F (5'-CTIGGICCIYTKCAYAC-3') and nosZ-II-R (5'-GCIGARCARAAITCBGTRC-3') according to a previously reported reaction mixture and program (Jones et al., 2013) with the minor

150   modification of using 10 μg of bovine serum albumin (BSA; Takara, Bio Inc.) instead of T4 gp32. PCR products were purified using an agarose gel DNA purification kit (Takara, Bio Inc.), ligated into the pMD19-T vector (Takara, Bio Inc.), and transformed into high-efficiency competent cells of *Escherichia coli* according to the manufacturer's instructions. Forty to 127 positive *nosZ* clones were randomly selected from each library, reamplified using the vector primers M13-F and RV-M, and sequenced using

155   ABI 3730 automated DNA sequence analyzer (Applied Biosystems). Poor-quality sequences with termination codons were manually checked and removed, and chimeras were removed using UCHIME (Edgar et al., 2011). All sequences were clustered into operational taxonomic units (OTUs) based on a 3% sequence divergence cutoff (Jones et al., 2014; Wittorf et al., 2020). The coverge (C) of each clone libarary was calculated by $C = 100\% [1 - (n / N)]$ (Mullins et al., 1995), where n is the number of unique

160   OTUs and N the total number of clones in a library. Alpha diversity indices (Shannon, Simpson, and Chao1) of the clade II-type *nosZ* gene were calculated using the Usearch package (Edgar et al., 2010). The representative sequences of OTUs were translated and analyzed with the BLASTp tool (*e*-value <10^{-5}). The top 10 most similar sequences of each OTU were used as references. The deduplicated reference sequences and the representative sequences of OTUs were aligned using MAFFT (Katoh and Standley,

165   2013) and automatically trimmed using trimAl (Capella-Gutiérrez et al., 2009). A maximum likelihood (ML) phylogenetic tree was constructed using Fasttree (v2.7.1, default parameters) (Price et al., 2010) with 500 bootstrap replicates for node support determination. The taxonomy of the OTU was assigned according to the phylogenetic relationship.

170   **2.3 Quantitative PCR of six functional genes**

Archaeal *amoA,* bacterial *amoA*, *nirS*, *nirK*, *nosZ* clade I, and *nosZ* clade II genes were quantified by qPCR with DNA and cDNA as templates using a CFX96 (Bio-Rad Laboratories, Singapore). Given the relatively high ammonia concentration in the estuaries, the ammonia-oxidizing archaea (AOA) shallow cluster (Water Column Cluster A; Francis et al., 2005) was targeted with the primer set Arch-amoAFA

and Arch-amoAR (Beman et al., 2008). Ammonia-oxidizing bacteria (AOB) are mostly affiliated with two groups: Betaproteobacteria (β-AOB) and Gammaproteobacteria (γ-AOB) (Lam et al., 2007). Since the latter was below detection limit in previous studies of Chinese estuaries (Zheng et al., 2017; Hou et al., 2018), only β-AOB was targeted with the primer set amoA-1F and amoA-r New (Rotthauwe and Witzel, 1997; Hornek et al., 2006). Bacterial *nirS* and *nirK* genes were quantified with the primer sets nirS-1F and nirS-3R (Braker et al., 1998) and nirK876 and nirK1040 (Henry et al., 2004). Bacterial clade I-type *nosZ* genes were quantified with the primer set nosZ2F and nosZ2R (Henry et al., 2006).

For the clade II-type *nosZ* gene quantification, the previously published primer sets were found to have less than 80% amplification efficiency (Jones et al., 2013, 2014; Chee-Sanford et al., 2020). Here, we designed a new primer set for use in our estuarine samples to quantify this gene. Representative nucleotide sequences of each OTU obtained from the clone libraries derived from the PRE samples (n=48) were translated into amino acid sequences and then aligned with the representative reference sequences (n=116; covering 87 genera) obtained from the Functional Gene Repository (http://fungene.cme.msu.edu/index.spr) by Clustal W. Two highly conserved regions containing five and three amino acids in length were chosen to design new primer fragments. The new primer pairs and the previously published nosZ-II-F and nosZ-II-R primer sets (Jones et al., 2013) were all evaluated by Primer Premier 6.0, and eligible primer sets (GC content: 40–60%; optimal melting temperatures: 52–58 °C; stable 5' end and specific 3' end with no clamp or complementary structure) were tested by qPCR. The best primer combination was nosZ-II-F and the newly designed reverse primer (nosZ-II-Rnew: KGCRTAGTGIGGYTCDCC) with a ~325 bp target fragment length (Fig. S1). The qPCR system is shown in Table S2, and the optimized qPCR program was as follows: an initial 5 min denaturing step at 95 °C, followed by 35 cycles of 95 °C for 30 s, annealing at 53 °C for 60 s, 72 °C extension for 60 s and a final extension at 72 °C for 10 min. The coverage of the primer sets was evaluated using the Search_pcr2 command of Usearch with the 116 reference sequences mentioned above and all clone sequences (n=1378) obtained from the clone libraries. A coverage of 93.5% (≤2 mismatches) was obtained for the new primer set.

The presence of PCR inhibitors in DNA extracts was examined by qPCR with different dilutions of DNA (1-, 10-, and 100-fold dilutions). The samples with inhibitor were diluted 10 times to overcome the

inhibitor effect according to our evaluation. Standard curves were constructed for the six genes using plasmid DNA from clone libraries generated from the PCR products. qPCRs were performed in triplicate and analyzed against a range of standards (10^1 to 10^8 copies per μL). All specific primer sequences, reactions, and programs for qPCR/PCR used in this study are shown in Table S2. The amplification efficiencies ranged from 87% to 109% with $R^2 > 0.99$ for each qPCR run. The specificity of qPCR products was verified by melting curves, agarose gel electrophoresis, and sequencing.

2.4 Statistical analysis

Redundancy analysis (RDA) based on qPCR or clone library data was used to analyze variations in the gene/transcription distribution and *nosZ* clade II community composition under environmental constraints using R (R Core Team, 2017). The qPCR or clone library-based relative abundances and environmental factors were normalized via Z transformation (Magalhães et al., 2008). The collinearity between environmental parameters was excluded (variance inflation factors > 10; Palacin-Lizarbe et al., 2019). The null hypothesis that the community structure was independent of environmental parameters was tested using constrained ordination with a Monte Carlo permutation test (999 permutations). Since a normal distribution of the individual datasets was not always met, we used the nonparametric Wilcoxon rank-sum tests for comparing two variables in GraphPad Prism software (San Diego, CA, USA). The bivariate correlations were described by Spearman's (ρ value) or Pearson's (r value) correlation coefficients. False discovery rate-based multiple comparison procedures were applied to evaluate the significance of multiple hypotheses and identify truly significant comparisons (false discovery rate-adjusted *P* value) (Pike, 2011).

3 Results

3.1 Environmental characteristics of the four estuaries

Water temperature increased with decreasing latitude from the BS (16.1–26.4 °C) to the YRE (19.2–29.1 °C) and JRE (28.7–30.8 °C), where samples were all collected in summer. Samples were collected in winter in the southernmost PRE, where the water temperature was 19.7–20.5 °C (Fig. 2). Salinity exhibited consistently high values in all sites of the BS and YRE (26.4–34.6 ppt), except for two low values (14.34 and 21.66 ppt) observed in the river mouth. In the JRE and PRE, obvious salinity gradients were detected from 0.1 to 30.7. The DO concentration varied in the range of 4.25–8.46 mg L^{-1} in the BS,

1.25–8.71 mg L^{-1} in the YRE, 4.04–6.89 mg L^{-1} in the JRE, and 2.22–9.22 mg L^{-1} in the PRE. There was a distinct DO gradient from upstream to downstream of the PRE (Fig. 2). The dissolved inorganic nitrogen (DIN: ammonium, nitrite, and nitrate) concentrations were generally lower in the BS and YRE compared to those in the JRE and PRE. The ammonium concentration was in the range of 0.006–1.27 µM in the BS, below detection (BD) to 1.99 µM in the YRE, 7.01–36.78 µM in the JRE, and 1.71–417.38 µM in the PRE. The nitrite concentration was in the range of BD–5.65 µM in the BS and 0.004–2.5 µM in the YRE, 7.24–30.87 µM in the JRE, and 0.41–69.23 µM in the PRE. The nitrate concentration ranged from 0.067–13.97 µM in the BS, 0.23–65.09 µM in the YRE, 24.94–241.32 µM in the JRE, and 3.0–320.53 µM in the PRE. Clear DIN concentration gradients were observed from upstream to downstream in the JRE and PRE, particularly in the PRE.

3.2 Distribution of six key functional genes

The abundances of archaeal *amoA*, bacterial *amoA*, *nirS*, *nirK*, *nosZ* I, and *nosZ* II genes showed distinct distribution patterns among the four estuaries (Figs. 3a–h). We divided the six genes into two groups for analysis: one group included archaeal and bacterial *amoA*, *nirS*, and *nirK* genes indicating nitrification and denitrification related to N_2O production (Figs. 3a–d), and the other included bacterial *nosZ* I and *nosZ* II genes indicating N_2O consumption (Figs. 3e–h). In the gene group of N_2O production-related processes, archaeal *amoA* was the most dominant in the BS (2.66×10^4–3.68×10^8 copies L^{-1}) and YRE (4.86×10^3–9.47×10^7 copies L^{-1}) (Wilcoxon test, $P < 0.01$; Figs. 3a, b and Table S3), accounting for 3.96% to 96.2% and 2.84% to 99.67% of N_2O production-related gene abundance, respectively. In contrast to the northern estuaries, archaeal *amoA* (5.28×10^5–4.40×10^6 copies L^{-1}) and bacterial *nirS* (2.57×10^5–6.29×10^6 copies L^{-1}) genes codominated the gene group of N_2O production-related processes in the JRE (Fig. 3c), accounting for 2.43% to 72.93% and 25.03% to 93.77%, respectively. In the southernmost PRE, the *nirS* gene was the most abundant (3.48×10^4–1.66×10^9 copies L^{-1}), especially upstream ($P < 0.05$), accounting for 4.24% to 99.91% (Fig. 3d). Generally, archaeal *amoA* was widespread in all samples, and its abundance decreased from north to south with differences of one to two orders of magnitudes. A similar pattern was observed for bacterial *amoA*, with lower abundances than archaeal *amoA* (Table S3). The abundance of the *nirS* gene was highest in the PRE among the four estuaries, while the highest number of copies of the *nirK* gene was present in the BS (Table S3). Among the different water depths,

only the bacterial *amoA* and *nirS* genes in the BS were observed to be more highly distributed in the middle and bottom layers than in the surface layer by one to three orders of magnitude ($P < 0.05$).

In the N_2O-consuming genes, the abundances of the clade II-type *nosZ* gene were 6.55×10^3 to 2.24×10^7 copies L^{-1} in the BS (Fig. 3e), 6.14×10^3 to 8.11×10^6 copies L^{-1} in the YRE (Fig. 3f), and BD to 1.17×10^7 copies L^{-1} in the PRE (Fig. 3h), outnumbering the clade I-type ($P < 0.01$), with no significant differences among the three estuaries. However, the clade II-type *nosZ* gene was below the detection limit in the JRE, and only the clade I-type was detected with a range of 7.15×10^3–2.32×10^5 copies L^{-1} (Fig. 3g and Table S3). The numbers of copies of the clade I-type *nosZ* gene were higher in the BS estuary than in the other three estuaries ($P < 0.01$).

3.3 Transcription activity of six key functional genes

For the four genes of N_2O production-related processes, a generally similar relative abundance distribution pattern was observed between transcripts and genes in the BS (Fig. 3i). Archaeal *amoA* gene transcripts (3.51×10^3–1.62×10^6 transcripts L^{-1}) were significantly more abundant than other transcripts ($P < 0.01$), accounting for 37.94% to 99.30% of the total abundance of gene transcripts (Table S4). Slightly different from the gene distribution in which the number of copies of the bacterial *amoA* gene was relatively more abundant than that of the archaeal *amoA* gene in the river mouth of the YRE (Fig. 3b), the archaeal *amoA* gene transcript was abundant in the whole YRE, accounting for 9.1% to 100% of the total abundance of gene transcripts, with a dominant abundance of *nirS* gene transcripts in a few samples (Fig. 3j). A different distribution pattern was also observed between transcripts and genes in the JRE (Figs. 3c, k). Bacterial *amoA* (7.06×10^5–8.22×10^7 transcripts L^{-1}) rather than archaeal *amoA* transcripts ($P < 0.05$) were codominant with *nirS* transcripts (5.96×10^5–2.31×10^7 transcripts L^{-1}) (Fig. 3k). Notably, the total gene transcript abundance of N_2O production-related processes was higher in the JRE (1.31×10^6–9.76×10^7 transcripts L^{-1}) than in the BS and YRE (3.03×10^2–1.12×10^6 transcripts L^{-1}) ($P < 0.01$; Table S4). Bacterial *amoA* gene transcripts, consistent with the gene distribution, significantly increased with depth in the BS ($P < 0.05$). No significant differences in transcript abundance were observed among different depths for the six functional genes in the YRE.

For the N_2O-consuming genes, only the clade I-type *nosZ* gene transcript was determined (26.2–2.34×10^3 transcripts L^{-1}), while the clade II-type *nosZ* gene transcript was below the detection limit in

the BS (Fig. 3l; Table S4). However, the *nosZ* II gene transcripts (bellow detection to 1.81×10^5 transcripts L^{-1}) dominated most stations in the YRE, except for a dominant distribution of the *nosZ* I gene transcript in the river mouth (Fig. 3m). Similar to the gene distribution, in the JRE, only the *nosZ* I gene transcript was determined (1.23×10^3–5.37×10^4 transcripts L^{-1}) (Fig. 3n). No RNA samples were obtained in the PRE.

3.4 Phylogenetic diversity of the clade II *nosZ* gene

Clone libraries of *nosZ* clade II were constructed for 19 samples from the four estuaries, resulting in a total of 1378 quality-controlled sequences that were clustered into 441 OTUs at a similarity level of 97%. The coverage of each clone library ranged from 73.9 to 96.2%. Higher gene diversity of *nosZ* clade II was observed in the water and sediment samples from the JRE and the sediment sample from the YRE than in the other samples (Fig. S2a). The rarefaction curves of the samples from JRE and the sediment sample from YRE did not reach a plateau (data not shown), suggesting that some of the diversity of *nosZ* clade II remained unsampled. Phylogenetic analysis of the representative sequences of all the OTUs indicated that the clade II *nosZ* gene sequences were grouped with Bacteroidetes, Proteobacteria, Actinobacteria, Chloroflexi, Chlorobi, Ignavibacteriae, Gemmatimonadetes, Cyanobacteria, and Acidobacteria, in which the OTUs affiliated with Bacteroidetes, Proteobacteria, Chloroflexi, and Actinobacteria were generally abundant among all samples (Fig. 4b). The OTUs belonging to Bacteroidetes were divided into two clusters according to the topological structure of the phylogenetic tree. One cluster contained the reference sequences mainly from marine habitats and the OTU sequences retrieved from the four estuaries, while the other cluster included the reference sequences mainly from terrestrial habitats and the OTU sequences retrieved only from the low-latitude subtropical estuaries JRE and PRE. The OTU sequences affiliated with Alpha-, Gamma-, Delta-, Epsilonproteobacteria, and Actinobacteria were retrieved from the four estuaries, and the reference sequences were mainly from marine habitats, while the OTUs related to Betaproteobacteria, Oligoflexia, Chlorobi, and *Candidatus Melainabacteria* were retrieved only from the subtropical estuaries (JRE and PRE), and the reference sequences were mainly from terrestrial habitats (Fig. 4a). Most known clusters of *nosZ* clade II can be found in our libraries, including a recently identified widespread clade II-type *nosZ* gene affiliated with the class Oligoflexia (Nakai et al., 2014).

320   A community structure shift of *nosZ* clade II was observed among the four estuaries (Fig. 4b).

Bacteroidetes was the most dominant group in the samples from the BS (39.0–68.5%), followed by

Proteobacteria (Gamma-, Delta-, and Alphaproteobacteria; 18.7–26.0%). The sequences

phylogenetically grouped into Proteobacteria (Gamma-, Delta-, and Epsilonproteobacteria; 23.0–70.6%)

dominated the clone libraries from the YRE, followed by Chloroflexi (6.9–47.3%). The sequences from

325   the JRE were also mainly affiliated with Proteobacteria (Beta-, Gamma-, Delta-, and Alphaproteobacteria

and Oligoflexia; 11.8–40.5%), Bacteroidetes (30.9–37.9%), and Chloroflexi (12.1–50.9%). In contrast

to the three estuaries, the sequences affiliated with Bacteroidetes were absolutely dominant in the clone

libraries of the PRE (>69.2%). A nonmetric multidimensional scaling (NMDS) analysis indicated that

nosZ clade II communities from the same estuary were clustered together at a >10% Bray-Curtis

330   similarity level, except for a separate cluster of the sediment community from the YRE (Fig. S2b). The

nosZ clade II communities from the southern estuaries (JRE and PRE) and northern estuaries (YRE and

BS) were clustered separately at a >3% Bray-Curtis similarity level.

3.5 Correlations between six key functional genes and environmental factors

335   Variations in the gene/transcript distributions under environmental constraints were analyzed by RDA.

The first two RDA axes explained 19.98% and 5.36% of the total variation in the gene‑environment

relationship (Fig. 5a). Salinity, DO, nitrite, and ammonium concentrations were significantly correlated

with gene distribution ($P < 0.01$). The main variation in N_2O source or sink process-related genetic

potentials was across a *nirS* vs. archaeal *amoA* abundance gradient. The *nirS*-rich samples corresponded

340   to those from the southern estuaries (JRE and PRE) with higher ammonium and nitrite concentrations.

In contrast, the samples with the highest abundance of archaeal *amoA* were located in sites with high

salinity and low ammonium concentrations in the northern estuaries (BS and YRE). Notably, RDA of

the gene transcripts and environmental variables clearly separated the transcripts from different estuaries

along the axes, which explained 26.4% and 8.27% of the total variation (Fig. 5b). Variation in transcript

345   distribution was significantly correlated with pH, temperature, nitrite, and nitrate concentration ($P <$

0.01). The main variation of these transcripts was distributed across archaeal and bacterial *amoA* vs. *nosZ*

clade II abundance gradients. The archaeal *amoA* transcript-rich samples corresponded to those from the

BS and YRE sites with lower temperatures. The bacterial *amoA* gene was actively transcribed in the JRE

and positively correlated with nitrite and nitrate concentrations. The *nosZ* clade II transcript-rich samples

350 corresponded to those from the YRE sites with relatively higher pH and temperature. The *nosZ* clade I

and *nirS* transcript distributions were also positively correlated with pH and temperature, respectively.

RDA based on the clone library data of the clade II-type *nosZ* gene revealed that the *nosZ* II

community composition was significantly affected by temperature ($P < 0.01$; Fig. 5c). The first two RDA

axes explained 33.29% and 13.24% of the total variation. The *nosZ* II gene community compositions in

355 the BS may prefer environments with relatively high salinity and temperature. The community

compositions in the JRE water may prefer environments with a high temperature (the sediment samples

were not included in this analysis due to a lack of biogeochemical parameters). The *nosZ* clade II

microbes in the PRE and YRE may prefer to distribute in environments with high ammonium

concentrations.

360

4 Discussion

4.1 Niche differentiation of functional genes controlled by environmental factors

There was a distinct large-scale spatial structure among the detected genes, as shown in Fig. 3. The

different sampling seasons between the PRE (January) and the other three estuaries (June to September)

365 may influence the spatial distribution of functional genes across the four estuaries. However, the niche

differentiation of functional genes, spatially or temporally, is controlled by environmental factors in

essence, such as temperature, salinity, oxygen and nutrient availabilities, and primary productivity.

Comparing the relative contributions of these functional genes to the total number of gene copies across

the study regions, there was a strong negative correlation between the relative abundances of the archaeal

370 *amoA* gene and bacterial *nirS* gene ($\rho = -0.89$, $P < 0.01$), and they showed contrasting patterns along

salinity and DIN gradients (Fig. S3). Samples from the BS and YRE exhibited high salinity and low DIN

concentrations. The high abundance of the archaeal *amoA* gene in these areas is consistent with previous

findings of nitrifiers comprised predominantly of AOA in estuarine environments with higher salinity

and lower ammonia concentrations because archaeal nitrifiers exhibit a high ammonia affinity and

375 salinity tolerance (Martens-Habbena et al., 2009; Abell et al., 2010; Bernhard et al., 2010; Zhang et al.,

2014; Hou et al., 2018; Hink et al., 2018; Ma et al., 2019). In contrast, both the JRE and PRE are typical

subtropical eutrophic estuaries with high DIN inputs from surrounding environments (Cao et al., 2005;

He et al., 2014; Yan et al., 2012b). Denitrifying bacteria are more adaptable to environments with high

organic carbon and nitrogen concentrations because they usually have high requirements for substrates

380 (Braker et al., 2000; Smith et al., 2007; Mosier and Francis, 2010; Wang et al., 2014; Wei et al., 2015;

Lee and Francis, 2017). The presence of nitrogen oxides was also shown to activate *nirK* and *nirS* gene

expression under anoxic conditions (Riya et al., 2017). Thus, the *nirS*-containing group was more

abundant upstream of the JRE and PRE. The significant correlations between DIN and the *nirS* gene (Fig.

S3) and transcript ($\rho = 0.341$, $P < 0.01$; data not shown) are consistent with a previous conclusion that

385 high anthropogenic N loading stimulates denitrification (Beaulieu et al., 2011; Cole and Caraco, 2001;

Garnier et al., 2006; Yan et al., 2012a).

Previous studies of N_2O-consuming gene abundance have mainly focused on terrigenous

ecosystems, e.g., in soil samples, the clade I- and II-type *nosZ* genes ranged from 10^4 to 10^8 and 10^4 to

10^7 copies g dry soil^{-1}, respectively (Jones et al., 2013, 2014). In marine ecosystems, only the oxygen-

390 depleted waters and coastal sediments have been investigated, where the clade I-type was approximately

10^5 copies L^{-1} and both clades I and II ranged from 10^5–10^7 copies g wet sediment^{-1}, respectively (Wittorf

et al., 2020; Sun et al., 2021). We detected that the number of copies of the *nosZ* gene ranged from

6.59×10^3 to 2.35×10^8 copies L^{-1}, with an average of 4.94×10^6 copies L^{-1}, in China's estuarine and coastal

areas. There was a strong negative correlation between the relative abundance of the clade I- and II-type

395 *nosZ* genes ($\rho = -1$, $P < 0.01$), indicating that the two types were affiliated with different groups. The

distribution of *nosZ* (clades I and II) gene transcripts was significantly positively correlated with pH (Fig.

5b), suggesting that acidification of the ocean may decrease N_2O consumption potential. N_2O production

influenced by pH has been observed in N-cycling water engineering systems and terrestrial ecosystems

(Mørkved et al., 2007; Blum et al., 2018). Therefore, some studies suggest that liming for acidic soils

400 could mitigate N_2O emissions (McMillan et al., 2016; Wang et al., 2017; Senbayram et al., 2019). The

nosZ genes and transcripts showed significantly negative correlations with nitrate and/or nitrite (Fig. 5a

and b), and similar correlations were also found in mountain lake habitats (Palacin-Lizarbe et al., 2019).

It is possible that high abundances of *nosZ* gene and transcript lead to high consumption of nitrate and

nitrite. In addition, it was reported that the presence of nitrate can inhibit the reduction of N_2O to N_2

405 (Blackmer and Bremner, 1978). DO also showed an important influence on denitrifying genes, which is

consistent with a previous conclusion that O_2 concentration can impact the expression and metabolism of denitrification genes through protein sensing of oxygen conditions (Qu et al., 2016; Riya et al., 2017). Notably, we found that the distribution and abundance of the *nosZ* gene and the *nirS* or *nirK* genes were distinctly different, indicating that these functional genes were affiliated with different denitrifiers. This

410   may be because not all N_2O-consuming bacteria contain all denitrification genes (Sanford et al., 2012).

4.2 Gene transcription expression controlled by environmental factors

The gene transcript abundance showed a certain regional distribution difference with gene abundance (Fig. 3), suggesting that environmental factors might have different influences on gene distribution and

415   transcript activity. The bacterial *amoA* gene was transcribed actively in the JRE, although the archaeal *amoA* gene prevailed in gene abundance. Frequent water exchange may result in a large amount of the archaeal *amoA* gene from the ocean, but AOB are more active under high ammonium and low salinity conditions. AOB have been indicated to be the primary N_2O producer, even in an AOA-dominated environment (Meinhardt et al., 2018). A meta-analysis also revealed that AOB respond more strongly

420   than AOA to nitrogen addition (Carey et al., 2016). High abundances of bacterial *amoA* and *nirS* gene transcripts make the JRE a more potentially active area of N_2O production compared to the northern estuarine and coastal areas, which may be attributed to its high nitrogen input from surrounding environments. In contrast, in the mouth of the YRE, although the bacterial *amoA* gene contributed a large proportion of the gene abundance, the archaeal *amoA* gene was transcribed more actively. Flushing water

425   from the Yangtze River may transport a large amount of the bacterial *amoA* gene, but the archaeal *amoA* gene is more competitive in low ammonium and oxygen environments (Fig. 2) since the enzyme ammonia monooxygenase in AOA has a higher affinity for ammonia and a lower oxygen requirement than the AOB (Park et al., 2010; Martens-Habbena and Stahl, 2011). The *nosZ* clade I gene was transcribed more actively even though the *nosZ* clade II gene was more abundant (e.g., the case in the

430   BS shown in Fig. 3e and l). The higher growth yields of clade II-type N_2O-reducing bacteria than those of clade I-type (Yoon et al., 2016) may lead to a preponderance of the *nosZ* clade II gene. However, a microbial culture of clade I-type N_2O-reducing bacteria has been reported to have the capability of continually synthesizing N_2O reductase enzyme under oxic conditions to allow for a rapid transition into

anoxic environments (Lycus et al., 2018). Such a strategy could result in the more abundant *nosZ* clade I transcripts observed in the estuaries.

4.3 N$_2$O emissions potential implied by functional gene distribution

The community structure of nitrifiers and denitrifiers is thought to have an important influence on N$_2$O emissions. For example, the abundance and expression of the archaeal *amoA* gene showed comparable patterns with N$_2$O production in the OMZ of the eastern tropical North Atlantic (Löscher et al., 2012). Reduction of the abundance of bacterial *amoA* genes in hyperthermophilic composting was proven to decrease N$_2$O emissions (Cui et al., 2019). The expression of the *nirK* gene induced by the addition of nitrate caused an increase in N$_2$O production in an anoxic soil slurry experiment (Riya et al., 2017). Transcription of clade I-type *nosZ* mRNA in the lower N$_2$O emission system was one order of magnitude higher than that in the higher N$_2$O emission system in wastewater treatment plants (Song et al., 2014). To assess how community structure controls the regional N$_2$O source or sink potential across China's estuaries, we collected the data on N$_2$O concentration, N$_2$O flux, and ΔN$_2$O in the four estuaries from the literature, covering January to November from 2002 to 2015 (Table S5; Chen et al., 2008; Lin et al., 2016, 2020; Ma et al., 2019; Song et al., 2015; Wang et al., 2014, 2016; Wu et al., 2013; Xu et al., 2005; Zhan et al., 2011; Zhang et al., 2008, 2010), and analyzed their relationships with the six functional gene distributions. The N$_2$O concentration, N$_2$O flux, and ΔN$_2$O all showed an increasing distribution pattern from the northern, high-latitude to the southern, low-latitude estuaries (Figs. 6a–c), with hot spots in the north and center of the BS, nearshore of the YRE, and upstream of the JRE and PRE. Notably, total *amoA* gene abundances displayed a contrary pattern, while total *nir* gene abundances and the ratio of total *nir* to *amoA* gene abundances (*nir*/*amoA*) had generally consistent patterns with the N$_2$O concentration, N$_2$O flux, and ΔN$_2$O across the four estuaries (Figs. 6d–f). A significant correlation was even observed between the N$_2$O flux and the *nir*/*amoA* ratio based on the four averages of the four estuaries (r = 0.95, n = 4, $P < 0.05$). Therefore, the *nir*/*amoA* ratio can indicate the N$_2$O emission potential in China's estuaries, which is consistent with previous findings that the N$_2$O production yield of denitrification is higher than that of nitrification in the lab and in situ experiments (Frey et al., 2019; Kester et al., 1997; Löscher et al., 2012; Stieglmeier et al., 2014).

Notably, the total *nosZ* gene abundance of N$_2$O-reducing denitrifiers seemed to have a contrasting distribution pattern with the N$_2$O concentration, N$_2$O flux, and ΔN$_2$O across the four estuaries, with higher abundances in the high-latitude BS and lower abundances in the low-latitude JRE (Fig. 6g). The

465   total *nosZ* gene abundances were one to two orders of magnitude lower than the total *nir* gene abundances in the JRE and PRE, where the N$_2$O concentration and flux were higher than those in the BS and YRE. This indicated a distinctly higher denitrification-derived N$_2$O emission potential in the JRE and PRE. The ratio of total *nir* to *nosZ* clade I gene abundances (*nir*/*nosZ* I) had a highly similar pattern with the N$_2$O concentration, N$_2$O flux, and ΔN$_2$O across the four estuaries in general (Fig. 6h), and significant

470   correlations were also observed between the N$_2$O flux and *nir*/*nosZ* I (r = 0.97, n = 4, $P < 0.05$). Therefore, the *nir*/*nosZ* I ratio could be a better indicator of N$_2$O emission potential in China's estuaries. Abundances and activities of the N$_2$O-producing (*nirS* or *nirK*–bearing) community relative to the N$_2$O-reducing (*nosZ*-bearing) community have also been used to assess the N$_2$O emission potential of soils (Thompson, 2016; Zhao et al., 2018). Similarly, the functional gene transcript distribution indicated that the *nir*/*nosZ*

475   I and *nir*/*amoA* gene transcript abundance ratios also had consistent patterns with the N$_2$O concentration, N$_2$O flux, and ΔN$_2$O across the four estuaries in general (Fig. S4). The high load of DIN in estuaries could be responsible for the high denitrification-derived N$_2$O emission potential. Both the *nir*/*nosZ* and *nir*/*amoA* ratios were positively correlated with the NH$_4^+$, NO$_3^-$, and NO$_2^-$ concentrations (Spearman's ρ = 0.32–0.68, n = 114–122, $P < 0.01$ for each) and negatively correlated with salinity (Spearman's ρ =

480   −0.45 – −0.66, n = 114–122, $P < 0.01$ for each). Previous studies in the YRE have proven that nitrogen input accelerates N$_2$O production in estuaries (Yan et al., 2012a; Zhang et al., 2010). Therefore, sufficient supplies of substrates may support high rates of denitrification and thus high N$_2$O emissions.

4.4 Influence of N$_2$O emissions by N$_2$O reducer composition

485   The community structure and diversity of the clade II *nosZ* gene retrieved from China's estuaries are different from those previously reported in soil and marine OMZ water (Jones et al., 2013, 2014; Sun, 2021). The dominant *nosZ* clade II-bearing groups are affiliated with Bacteroidetes, Chloroflexi, Gamma-, and Betaproteobacteria in our four estuarine and coastal areas. However, the most abundant *nosZ* clade II groups found in the OMZs of the eastern tropical South and North Pacific and the Arabian

490   Sea are affiliated with *Anaeromyxobacter* (Deltaproteobacteria) (Sun et al., 2017; Sun et al., 2021) and

those in the coastal OMZ waters of the Golfo Dulce, Costa Rica are affiliated with Gammaproteobacteria, Marinimicrobia, Bacteroidetes, and SAR324 (Bertagnolli et al., 2020). The *nosZ* clade II organisms from terrestrial systems show distinctly higher diversity (Sanford et al., 2012; Jones et al., 2014; Hallin et al., 2018; Zhao et al., 2018; Kato et al., 2018). The phylogenetically distinct predominant N_2O reducers can

495   influence N_2O emissions directly or indirectly (Song et al., 2014). According to genomic information, *nosZ* clade II carriers affiliated with Deltaproteobacteria and Chlorobi have neither the *nirK* nor *nirS* gene, and less than half of *nosZ* clade II organisms affiliated with Bacteroidetes, Chloroflexi, Gamma-, and Epsilonproteobacteria harbor the *nirK* or *nirS* gene, while all of the *nosZ* clade II microbes affiliated with Alpha- and Betaproteobacteria also have the *nirS* gene (Hallin et al., 2018). Therefore, the distinct

500   *nosZ* clade II community structure among the four estuaries may contribute to their different N_2O emissions potential. For example, distinctly high diversity of the *nosZ* clade II gene was retrieved from the JRE water and sediment samples as well as the YRE sediment sample compared to the other estuaries. The high diversity of the *nosZ* clade II gene may be caused by the high temperature (e.g., in the low-latitude JRE) and sufficient nutrients at those sites. Previous studies have also indicate that the

505   biodiversity of denitrifying bacteria increases in high-temperature seasons (Castellano-Hinojosa et al., 2017) and that nitrogen availability has a positive effect on denitrifying bacteria in boreal lakes (Rissanen et al., 2011). In addition, the habitat type may also affect the abundance and diversity of N_2O-reducing communities, e.g., silty mud and sandy sediments have higher genetic potentials for N_2O reduction than cyanobacterial mat and *Ruppia maritima* meadow sediments (Wittorf et al., 2020).

510

5 Summary

This study revealed the distinct distribution patterns of six key microbial functional genes and transcripts related to N_2O production and consumption pathways in the BS, the YRE, the adjacent ECS, the JRE, and the PRE. The archaeal *amoA* genes and transcripts were more abundant in the northern BS, YRE,

515   and the adjacent ECS, while the denitrifier *nirS* genes and transcripts were more abundant in the southern JRE and PRE. The *nosZ* clade II gene was more abundant than the clade I-type throughout the estuaries except for in the JRE and a few sites of the BS, while the opposite transcript distribution pattern was observed in these two estuaries. Water mass parameters (temperature and salinity), substrates (ammonia/ammonium, nitrite, and nitrate), and influencing parameters of substrate availability (DO and

pH) regulated the gene, transcript, and community composition distribution patterns. The community structure of the clade II-type *nosZ* gene retrieved from China's estuaries was distinctly different from those of the soil and marine OMZ. Furthermore, combined with the N_2O concentration, flux, and ΔN_2O data collected from previous studies, our analysis found that although both the clade I- and II-type *nosZ* genes of N_2O reducers were widely distributed in these estuaries, N_2O production by the denitrification pathway may be more important in determining the N_2O emissions patterns across the estuaries. Nitrogen loads may influence the N_2O source and sink processes by regulating the distribution of the related functional microbial groups.

Data availability

All quality-controlled sequences were submitted to GenBank with accession numbers OM567739– OM568649. All other data can be accessed in the form of Excel spreadsheets via the corresponding author.

Supplement

The Supplement related to this article is available online.

Author contributions

YZ conceived and designed the study. XD, XW, MC, ET, and NC performed the experiments and auxiliary data collection. XD analyzed the data. XD and YZ wrote the paper. All authors contributed to the interpretation of the results and critical revision.

Competing interests

The authors declare no conflicts of interest.

Acknowledgments

We thank Zuhui Zuo, Yufang Li, and Minyuan Liu for their assistance in sampling and DNA/RNA extraction, as well as Jiaming Shen for his valuable comments and suggestions in the preparation of the manuscript. Thanks are also given to CEES Open Cruise for the Jiulong River Estuary - Xiamen Bay and Shuiying Huang and Jiezhong Wu for their organizational help.

Financial support

This research was supported by the NSFC projects (42125603, 41721005, 92051114, and 42188102).

References

555   Abell, G. C. J., Revill, A. T., Smith, C., Bissett, A. P., Volkman, J. K., and Robert, S. S.: Archaeal ammonia oxidizers and *nirS*-type denitrifiers dominate sediment nitrifying and denitrifying populations in a subtropical macrotidal estuary, ISME J, 4(2), 286–300, doi:10.1038/ismej.2009.105, 2010.

Babbin, A. R., Bianchi, D., Jayakumar, A., and Ward, B. B.: Rapid nitrous oxide cycling in the suboxic ocean, Science., 348(6239), 1127–1129, doi:10.1126/science.aaa8380, 2015.

560   Bange, H. W., Rapsomanik, S., and Andreae, M. O.: Nitrous oxide in coastal waters, Global Biogeochem. Cycles, 10(1), 197–207, doi:10.1029/95GB03834, 1996.

Barnes, J. and Upstill-Goddard, R. C.: N$_2$O seasonal distributions and air-sea exchange in UK estuaries: Implications for the tropospheric N$_2$O source from European coastal waters, J. Geophys. Res. Biogeosciences, 116(1), doi:10.1029/2009JG001156, 2011.

565   Beaulieu, J. J., Tank, J. L., Hamilton, S. K., Wollheim, W. M., Hall, R. O., Mulholland, P. J., Peterson, B. J., Ashkenas, L. R., Cooper, L. W., Dahm, C. N., Dodds, W. K., Grimm, N. B., Johnson, S. L., McDowell, W. H., Poole, G. C., Maurice Valett, H., Arango, C. P., Bernot, M. J., Burgin, A. J., Crenshaw, C. L., Helton, A. M., Johnson, L. T., O'Brien, J. M., Potter, J. D., Sheibley, R. W., Sobota, D. J. and Thomas, S. M.: Nitrous oxide emission from denitrification in stream and river networks, Proc. Natl.

570   Acad. Sci. U. S. A., 108(1), 214–219, doi:10.1073/pnas.1011464108, 2011.

Beman, J. M., Popp, B. N., and Francis, C.: Molecular and biogeochemical evidence for ammonia oxidation by marine Crenarchaeota in the Gulf of California, ISME J. 2, 429–441, doi:10.1038/ismej.2008.33, 2008.

Bernhard, A. E., Landry, Z. C., Blevins, A., De La Torre, J. R., Giblin, A. E. and Stahl, D. A.: Abundance

575   of ammonia-oxidizing archaea and bacteria along an estuarine salinity gradient in relation to potential nitrification rates, Appl. Environ. Microbiol., 76(4), 1285–1289, doi:10.1128/AEM.02018-09, 2010.

Bertagnolli, A. D., Konstantinidis, K. T. and Stewart, F. J.: Non-denitrifier nitrous oxide reductases dominate marine biomes, Environ. Microbiol. Rep., 12(6), 681–692, doi:10.1111/1758-2229.12879, 2020.

580   Blackmer AM, Bremner JM.: Inhibitory effect of nitrate on reduction of N_2O to N_2 by soil microorganisms, Soil Biol Biochem., 10(3):187–191, doi:10.1016/0038-0717(78)90095-0, 1978.

Blum, J. M., Su, Q., Ma, Y., Valverde-Pérez, B., Domingo-Félez, C., Jensen, M. M. and Smets, B. F.: The pH dependency of N-converting enzymatic processes, pathways and microbes: effect on net N_2O production, Environ. Microbiol., 20(5), 1623–1640, doi:10.1111/1462-2920.14063, 2018.

585   Braker, G., Zhou, J., Wu, L., Devol, A. H. and Tiedje, J. M.: Nitrite reductase genes (*nirK* and *nirS*) as functional markers to investigate diversity of denitrifying bacteria in Pacific northwest marine sediment communities, Appl. Environ. Microbiol., 66(5), 2096–2104, doi:10.1128/AEM.66.5.2096-2104, 2000.

Brase, L., Bange, H. W., Lendt, R., Sanders, T. and Dähnke, K.: High resolution measurements of nitrous oxide (N_2O) in the Elbe estuary, Front. Mar. Sci., 4, doi:10.3389/fmars.2017.00162, 2017.

590   Cao, W., Hong, H. and Yue, S.: Modelling agricultural nitrogen contributions to the Jiulong River estuary and coastal water, Glob. Planet. Change, 47(2-4 SPEC. ISS.), 111–121, doi:10.1016/j.gloplacha.2004.10.006, 2005.

Capella-Gutiérrez, S., Silla-Martínez, J. M. and Gabaldón, T.: trimAl: A tool for automated alignment trimming in large-scale phylogenetic analyses, Bioinformatics, 25(15), 1972–1973, 595   doi:10.1093/bioinformatics/btp348, 2009.

Carey, C. J., Dove, N. C., Beman, J. M., Hart, S. C. and Aronson, E. L.: Meta-analysis reveals ammonia-oxidizing bacteria respond more strongly to nitrogen addition than ammonia-oxidizing archaea, Soil Biol. Biochem., 99, 158–166, doi:10.1016/j.soilbio.2016.05.014, 2016.

Castellano-Hinojosa, A., Correa-Galeote, D., Carrillo, P., Bedmar, E. J. and Medina-Sánchez, J. M.: 600   Denitrification and biodiversity of denitrifiers in a High-Mountain Mediterranean Lake, Front. Microbiol., 8, 1911, doi:10.3389/fmicb.2017.01911, 2017.

Chen, C. A., Wang, S., Lu, X., Zhang, S., Lui, H., Tseng, H., Wang, B. and Huang, H.: Hydrogeochemistry and greenhouse gases of the Pearl River, its estuary and beyond, Quaternary International, 186, 79–90, doi:10.1016/j.quaint.2007.08.024, 2008.

605   Chen, C. T. A.: Chemical and physical fronts in the Bohai, Yellow and East China seas, J. Mar. Syst., 78(3), 394–410, doi:10.1016/j.jmarsys.2008.11.016, 2009.

Codispoti, L. A. and Christensen, J. P.: Nitrification, denitrification and nitrous oxide cycling in the eastern tropical South Pacific ocean, Mar. Chem., 16(4), 277–300, doi:http://dx.doi.org/10.1016/0304-4203(85)90051-9, 1985.

610   Cole, J. J. and Caraco, N. F.: Emissions of nitrous oxide (N_2O) from a tidal, freshwater river, the Hudson River, New York, Environ. Sci. Technol., 35(6), 991–996, doi:10.1021/es0015848, 2001.

Conthe, M., Wittorf, L., Kuenen, J. G., Kleerebezem, R., Van Loosdrecht, M. C. M. and Hallin, S.: Life on N_2O: Deciphering the ecophysiology of N_2O respiring bacterial communities in a continuous culture, ISME J., 12(4), 1142–1153, doi:10.1038/s41396-018-0063-7, 2018.

615   Cui, P., Chen, Z., Zhao, Q., Yu, Z., Yi, Z., Liao, H. and Zhou, S.: Hyperthermophilic composting significantly decreases N_2O emissions by regulating N_2O-related functional genes, Bioresour. Technol., 272(1), 433–441, doi:10.1016/j.biortech.2018.10.044, 2019.

Dai, M., Wang, L., Guo, X., Zhai, W., Li, Q., He, B. and Kao, S. J.: Nitrification and inorganic nitrogen distribution in a large perturbed river/estuarine system: The Pearl River Estuary, China, Biogeosciences, 620   5(5), 1227–1244, doi:10.5194/bg-5-1227-2008, 2008.

Dai, M., Gan, J., Han, A., Kung, H. S. and Yin, Z.: Physical dynamics and biogeochemistry of the Pearl River plume, Biogeochem. Dyn. Major River-Coastal Interfaces, 321–352, doi:10.1017/cbo9781139136853.017, 2013.

Dang, H., Li, J., Chen, R., Wang, L., Guo, L., Zhang, Z. and Klotz, M. G.: Diversity, abundance, and 625   spatial distribution of sedimet ammonia-oxidizing Betaproteobacteria in response to environmental gradients and coastal eutrophication in Jiaozhou Bay, China, Appl. Environ. Microbiol., 76(14), 4691–4702, doi:10.1128/AEM.02563-09, 2010.

Domeignoz-Horta1, L. A., , AyméSpor 1, D. B., Breuil1, M.-C. and , Florian Bizouard1, J. L. and L. P.: The diversity of the N_2O reducers matters for the $N_2O:N_2$ denitrification end-product ratio across an 630   annual and a perennial cropping system, Front. Microbiol, 6:971, doi:10.3389/fmicb.2015.00971, 2015.

Edgar, R.C: Search and clustering orders of magnitude faster than BLAST, Bioinformatics, 26, 2460–2461, doi:10.1093/bioinformatics/btq, 2010.

Fayazbakhsh, K., Abedian, A., Manshadi, B. D. and Khabbaz, R. S.: Introducing a novel method for materials selection in mechanical design using Z-transformation in statistics for normalization of material properties, Mater. Des., 30(10), 4396–4404, doi:10.1016/j.matdes.2009.04.004, 2009.

Francis, C. A., Roberts, K. J., Beman, J. M., Santoro, A. E. and Oakley, B. B.: Ubiquity and diversity of ammonia-oxidizing archaea in water columns and sediments of the ocean, Proc. Natl. Acad. Sci. U. S. A., 102(41), 14683–14688, doi:10.1073/pnas.0506625102, 2005.

Frey, C., Bange, H. W., Achterberg, E. P., Jayakumar, A. and Carolin, R.: Regulation of nitrous oxide production in low oxygen waters off the coast of Peru, Biogeosciences, doi:10.5194/bg-17-2263-2020, 2020.

Garnier, J., Cébron, A., Tallec, G., Billen, G., Sebilo, M. and Martinez, A.: Nitrogen behaviour and nitrous oxide emission in the tidal Seine River estuary (France) as influenced by human activities in the upstream watershed, Biogeochemistry, 77(3), 305–326, doi:10.1007/s10533-005-0544-4, 2006.

Graf, D.R.; Jones, C.M.; Hallin, S.: Intergenomic comparisons highlight modularity of the denitrification pathway and underpin the importance of community structure for N_2O emissions, PLoS ONE, doi:10.1371/journal.pone.0114118, 2014.

Hallin, S., Philippot, L., Löf, F. E., Sanford, R. A. and Jones, C. M.: Genomics and ecology of novel N_2O-Reducing microorganisms, Trends Microbiol., 26, 43–55, doi:10.1016/j.tim.2017.07.003, 2018.

He, B., Dai, M., Zhai, W., Guo, X. and Wang, L.: Hypoxia in the upper reaches of the Pearl River Estuary and its maintenance mechanisms: A synthesis based on multiple year observations during 2000-2008, Mar. Chem., 167(July), 13–24, doi:10.1016/j.marchem.2014.07.003, 2014.

Henry, S., Bru, D., Stres, B., Hallet, S., and Philippot, L.: Quantitative detection of the *nosZ* gene, encoding nitrous oxide reductase, and comparison of the abundances of 16S rRNA, *narG*, *nirK*, and *nosZ* genes in soils, Appl. Environ. Microbiol., 72(8), 5181–5189, doi:10.1128/AEM.00231-06, 2006.

Hou, L., Xie, X., Wan, X., Kao, S. J., Jiao, N., and Zhang, Y.: Niche differentiation of ammonia and nitrite oxidizers along a salinity gradient from the Pearl River estuary to the South China Sea, Biogeosciences, 15(16), 5169–5187, doi:10.5194/bg-15-5169-2018, 2018.

Ji, Q., Buitenhuis, E., Suntharalingam, P., Sarmiento, J. L. and Ward, B. B.: Global nitrous oxide

660   production determined by oxygen sensitivity of nitrification and denitrification, Global Biogeochem.

Cycles, 32(12), 1790–1802, doi:10.1029/2018GB005887, 2018a.

Ji, Q., Frey, C., Sun, X., Jackson, M., Lee, Y., Jayakumar, A., Jeffrey, C. and Ward, B. B.: Nitrogen and

oxygen availabilities control water column nitrous oxide production during seasonal anoxia in the

Chesapeake Bay, Biogeosciences, 15, 6127–6138, doi:10.5194/bg-15-6127-2018, 2018b.

665   Jones, C. M., Graf, D. R. H., Bru, D., Philippot, L., and Hallin, S.: The unaccounted yet abundant nitrous

oxide-reducing microbial community: a potential nitrous oxide sink, ISME J. 7, 417–26,

doi:10.1038/ismej.2012.125, 2013.

Jones, C. M., Spor, A., Brennan, F. P., Breuil, M., Bru, D., Lemanceau, P., et al.: Recently identified

microbial guild mediates soil N_2O sink capacity, Nat. Climate change. 4, 801–805,

670   doi:10.1038/nclimate2301, 2014.

Jones, C. M., Stres, B., Rosenquist, M., and Hallin, S.: Phylogenetic analysis of nitrite, nitric oxide, and

nitrous oxide respiratory enzymes reveal a complex evolutionary history for denitrification, Mol. Biol.

Evol. 25, 1955–1966, doi:10.1093/molbev/msn146, 2008.

Katoh, K. and Standley, D. M.: MAFFT multiple sequence alignment software version 7: Improvements

675   in performance and usability, Mol. Biol. Evol., 30(4), 772–780, doi:10.1093/molbev/mst010, 2013.

Kester, R. A., De Boer, W., and Laanbroek, H. J.: Production of NO and N_2O by pure cultures of

nitrifying and denitrifying bacteria during changes in aeration, Appl. Environ. Microbiol., 63, 3872–3877,

doi:10.1128/AEM.63.10.3872–3877, 1997.

Lam, P., Jensen, M. M., Lavik, G., McGinnis, D. F., Müller, B., Schubert, C. J., Amann, R., Thamdrup,

680   B. and Kuypers, M. M. M.: Linking crenarchaeal and bacterial nitrification to anammox in the Black Sea,

Proc. Natl. Acad. Sci. U. S. A., 104(17), 7104–7109, doi:10.1073/pnas.0611081104, 2007.

Laperriere, S. M., Nidzieko, N. J., Fox, R. J., Fisher, A. W. and Santoro, A. E.: Observations of variable

ammonia oxidation and nitrous oxide flux in a eutrophic estuary, Estuaries and Coasts, 42(1), 33–44,

doi:10.1007/s12237-018-0441-4, 2019.

685   Lee, J. A., and Francis, C. A.: Spatiotemporal characterization of San Francisco Bay denitrifying communities: a comparison of *nirK* and *nirS* diversity and abundance, Microb. Ecol., 73(2), 271–284, doi:10.1007/s00248-016-0865-y, 2017.

Levipan, H. A., V. Molina, and C. Fernandez.: Nitrospina-like bacteria are the main drivers of nitrite oxidation in the seasonal upwelling area of the Eastern South Pacific (Central Chile ~36°S), Environ

690   Microbiol Rep., 6:565–73, doi:10.1111/1758-2229.12158, 2014.

Li, J., Nedwell, D. B., Beddow, J., Dumbrell, A. J., McKew, B. A., Thorpe, E. L. and Whitby, C.: *amoA* gene abundances and nitrification potential rates suggest that benthic ammonia-oxidizing bacteria and not archaea dominate N cycling in the Colne estuary, United Kingdom, Appl. Environ. Microbiol., 81(1), 159–165, doi:10.1128/AEM.02654-14, 2015.

695   Li, Z., Jin, W., Liang, Z., Yue, Y. and Lv, J.: Abundance and diversity of ammonia-oxidizing archaea in response to various habitats in Pearl River Delta of China, a subtropical maritime zone, J. Environ. Sci. (China), 25(6), 1195–1205, doi:10.1016/S1001-0742(12)60178-8, 2013.

Lin, J., Chen, N., Wang, F., Huang, Z., Zhang, X., and Liu, L.: Urbanization increased river nitrogen export to western Taiwan Strait despite increased retention by nitrification and denitrification, Ecol.

700   Indic., 109, 105756, doi:10.1016/j.ecolind.2019.105756, 2020.

Löscher, C. R., Kock, A., Könneke, M., Laroche, J., Bange, H. W., and Schmitz, R. A.: Production of oceanic nitrous oxide by ammonia-oxidizing archaea, Biogeosciences, 9, 2419–2429, doi:10.5194/bg-9-2419-2012, 2012.

Lu, Y., Cheung, S., Chen, L., Kao, S., Xia, X., Gan, J., et al.: New insight to niche partitioning and

705   ecological function of ammonia oxidizing archaea in subtropical estuarine ecosystem, Biogeosciences, 17, 6017–6032, doi:10.5194/bg-17-6017-2020, 2020.

Lycus P, Soriano-Laguna MJ, Kjos M, Richardson DJ, Gates AJ, Milligan DA, et al.: A bet-hedging strategy for denitrifying bacteria curtails their release of N_2O, Proc Natl Acad Sci USA, 2018;115:11820–5, doi:10.1073/pnas.1805000115, 2018.

710   Ma, L., Lin, H., Xie, X., Dai, M., and Zhang, Y.: Major role of ammonia-oxidizing bacteria in N_2O production in the Pearl River estuary, Biogeosciences, 16, 4765–4781, doi:10.5194/bg-16-4765-2019, 2019.

Marchant, H. K., Ahmerkamp, S., Lavik, G., Tegetmeyer, H. E., Graf, J., Klatt, J. M., Holtappels, M., Walpersdorf, E. and Kuypers, M. M. M.: Denitrifying community in coastal sediments performs aerobic

715   and anaerobic respiration simultaneously, ISME J. 11, 1799–1812, doi:10.1038/ismej.2017.51, 2017.

Martens-Habbena, W., and Stahl, D. A.: Nitrogen metabolism and kinetics of ammonia-oxidizing archaea, Methods Enzymol., 496, 465–487, doi:10.1016/B978-0-12-386489-5.00019-1, 2011.

Marzadri, A., Dee, M. M., Tonina, D., Bellin, A., and Tank, J. L.: Role of surface and subsurface processes in scaling N_2O emissions along riverine networks, Proc. Natl. Acad. Sci. U. S. A., 114(17),

720   4330–4335, doi:10.1073/pnas.1617454114, 2017.

Massana, R., Murray, A. E., Preston, C. M., and DeLong, E. F.: Vertical distribution and phylogenetic characterization of marine planktonic archaea in the Santa Barbara Channel, Appl. Environ. Microbiol., 63(1), 50–56, doi:10.1128/aem.63.1.50-56.1997, 1997.

Meinhardt, K. A., Stopnisek, N., Pannu, M. W., Strand, S. E., Fransen, S. C., Casciotti, K. L. and Stahl,

725   D. A.: Ammonia-oxidizing bacteria are the primary N_2O producers in an ammonia-oxidizing archaea dominated alkaline agricultural soil, Environ. Microbiol., 20(6), 2195–2206, doi:10.1111/1462-2920.14246, 2018.

Molina, V., Belmar, L., and Ulloa, O.: High diversity of ammonia-oxidizing archaea in permanent and seasonal oxygen-deficient waters of the Eastern South Pacific, Environ. Microbiol., 12: 2450–2465,

730   doi:10.1111/1462-2920.14246, 2010.

Mosier, A. C., and Francis, C. A.: Denitrifier abundance and activity across the San Francisco Bay estuary, Environ. Microbiol Rep., 2, 667–676, doi:10.1111/j.1758-2229.2010.00156.x, 2010.

Nakai, R., Nishijima, M., Tazato, N., Handa, Y., Karray, F., Sayadi, S., Isoda, H. and Naganuma, T.: *Oligoflexus tunisiensis* gen. nov., sp. nov., a Gram-negative, aerobic, filamentous bacterium of a novel

735   proteobacterial lineage, and description of *Oligoflexaceae* fam. nov., *Oligoflexales* ord. nov. and *Oligoflexia* classis nov, Int. J. Syst. Evol. Microbiol, 64, 3353–3359, doi:10.1099/ijs.0.060798-0, 2014.

Nevison, C., Butler, J. H., and Elkins, J. W.: Global distribution of N_2O and the ΔN_2O-AOU yield in the subsurface ocean, Global Biogeochem. Cycles, 17, 1–18, doi:10.1029/2003GB002068, 2003.

740 Palacin-Lizarbe, C., Camarero, L., Hallin, S., Jones, C., Caliz, J., Casamayor, E. O. and Catalan, J.: The DNRA-denitrification dichotomy differentiates nitrogen transformation pathways in mountain lake benthic habitats, Front. Microbiol., 10, 1229, doi:10.3389/FMICB.2019.01229, 2019.

Philippot, L.: Loss in microbial diversity affects nitrogen cycling in soil, ISME J., 11, 1609–1619, 2013.

Price, M. N., Dehal, P. S., and Arkin, A. P.: FastTree 2 - Approximately maximum-likelihood trees for large alignments, PLoS One 5, 9490, doi:10.1371/journal.pone.0009490, 2010.

745 Xu Jirong, Wang Youshao, Wang Qinji, Yin Jianping: Nitrous oxide concentration and nitrification and denitrification in Zhujiang River Estuary, China. J. Environ. Sci., 18, 4. 122–130, doi:, 2005.

Qu, Z., Bakken, L. R., Molstad, L., Frostegård, Å., and Bergaust, L. L.: Transcriptional and metabolic regulation of denitrification in Paracoccus denitrificans allows low but significant activity of nitrous oxide reductase under oxic conditions, Environ. Microbiol., 18, 2951–2963, doi:10.1111/1462-
750 2920.13128, 2016.

Ravishankara, A. R., Daniel, J. S. and Portmann, R. W.: Nitrous oxide (N_2O): The dominant ozone-depleting substance emitted in the 21st century, Science, 326(5949), 123–125, doi:10.1126/science.1176985, 2009.

Rissanen, A. J., Tiirola, M. and Ojala, A.: Spatial and temporal variation in denitrification and in the
755 denitrifier community in a boreal lake, Aquat. Microb. Ecol., 64(1), 27–40, doi:10.3354/ame01506, 2011.

Riya, S., Takeuchi, Y., Zhou, S., Terada, A. and Hosomi, M.: Nitrous oxide production and mRNA expression analysis of nitrifying and denitrifying bacterial genes under floodwater disappearance and fertilizer application, Environ. Sci. Pollut. Res., 24(18), 15852–15859, doi:10.1007/s11356-017-9231-y, 2017.

760 Rowley, G., Sullivan, M. J., Appia-Ayme, C., Gates, A. J. and Richardson, D. J.: Copper control of bacterial nitrous oxide emission and its impact on vitamin B12-dependent metabolism, Proc. Natl. Acad. Sci., 110(49), 19926–19931, doi:10.1073/pnas.1314529110, 2013.

Sanford, R. A., Wagner, D. D., Wu, Q. Z., Chee-Sanford, J. C., Thomas, S. H., Cruz-Garcia, C., Rodriguez, G., Massol-Deya, A., Krishnani, K. K., Ritalahti, K. M., Nissen, S., Konstantinidis, K. T. and
765 Loffler, F. E.: Unexpected nondenitrifier nitrous oxide reductase gene diversity and abundance in soils, Proc. Natl. Acad. Sci. U. S. A., 109(48), 19709–19714, doi:10.1073/Pnas.1211238109, 2012.

Santoro, A. E., Buchwald, C., McIlvin, M. R., and Casciotti, K. L.: Isotopic Signature of N_2O Produced by Marine Ammonia-Oxidizing Archaea, Science, 333, 1282–1285, doi:10.1126/science.1208239, 2011.

Sobarzo, M., Bravo, L., Donoso, D., Garcés-Vargas, J., and Schneider, W.: Coastal upwelling and seasonal cycles that influence the water column over the continental shelf off central Chile, Prog Oceanogr 75: 363–382., doi:10.1016/j.pocean. 2007. 08. 022, 2007.

Senbayram, M., Budai, A., Bol, R., Chadwick, D., Marton, L., Gündogan, R. and Wu, D.: Soil NO_3^- level and O_2 availability are key factors in controlling N_2O reduction to N_2 following long-term liming of an acidic sandy soil, Soil Biol. Biochem., 132(3), 165–173, doi:10.1016/j.soilbio.2019.02.009, 2019.

Shaw, L. J., Nicol, G. W., Smith, Z., Fear, J., Prosser, J. I., and Baggs, E. M.: *Nitrosospira spp*. can produce nitrous oxide via a nitrifier denitrification pathway, Environ. Microbiol., 8, 214–222, doi:10.1111/j.1462-2920.2005.00882.x, 2006.

Shcherbak, I., Millar, N., and Robertson, G. P.: Global metaanalysis of the nonlinear response of soil nitrous oxide (N_2O) emissions to fertilizer nitrogen, Proc. Natl. Acad. Sci., 111, 9199–9204, doi:10.1073/pnas.1322434111, 2014.

Silvennoinen, H., Liikanen, A., Torssonen, J., Florian Stange, C., and Martikainen, P. J.: Denitrification and nitrous oxide effluxes in boreal, eutrophic river sediments under increasing nitrate load: A laboratory microcosm study, Biogeochemistry, 91(2–3), 105–116, doi:10.1007/s10533-008-9262-z, 2008.

Smith, C. J., Nedwell, D. B., Dong, L. F., and Osborn, A. M.: Diversity and abundance of nitrate reductase genes (*narG* and *napA*), nitrite reductase genes (*nirS* and *nrfA*), and their transcripts in estuarine sediments, Appl. Environ. Microbiol., 73(11), 3612–3622, doi:10.1128/AEM.02894-06, 2007.

Song, D., Zhang, G., Li, P., and Liu, S.: Distribution and fluxes of nitrous oxide in the Bohai Sea in summer, Advances in Marine Sciences, 13–21, doi:10.12677/ams.2015.22003, 2015.

Song, K., Suenaga, T., Hamamoto, A., Satou, K., Riya, S., Hosomi, M. and Terada, A.: Abundance, transcription levels and phylogeny of bacteria capable of nitrous oxide reduction in a municipal wastewater treatment plant, J. Biosci. Bioeng., 118(3), 289–297, doi:10.1016/j.jbiosc.2014.02.028, 2014.

Stieglmeier, M., Mooshammer, M., Kitzler, B., Wanek, W., Zechmeister-Boltenstern, S., Richter, A. and Schleper, C.: Aerobic nitrous oxide production through N-nitrosating hybrid formation in ammonia-oxidizing archaea, ISME J., 8(5), 1135–1146, doi:10.1038/ismej.2013.220, 2014.

795   Sun, X., Amal Jayakumar., John C. Tracey., Elizabeth Wallace., Colette L. Kelly., Karen L. Casciotti., Bess B. Ward.: Microbial N_2O consumption in and above marine N_2O production hotspots, ISME, 15, 1434–1444, doi:10.1038/s41396-020-00861-2, 2021.

Sun, X., Jayakumar, A. and Ward, B. B.: Community composition of nitrous oxide consuming bacteria in the oxygen minimum zone of the Eastern Tropical South Pacific, Front. Microbiol., 8(JUN), 1–11,

800   doi:10.3389/fmicb.2017.01183, 2017.

Ter, C. J. F.: Canonical correspondence analysis: a new eigenvector technique for multivariate direct gradient analysis, Ecology, 67, 1167–1179, doi:10.2307/1938672, 1986.

Thompson, K.: Abundance, activity and community structure of nitrifier and denitrifier communities in Agro-Ecosystems, A Thesis presented to The University of Guelph, 2016.

805   Wang, L., Zhang, G., Zhu, Z., Li, J., Liu, S., Ye, W. and Han, Y.: Distribution and sea-to-air flux of nitrous oxide in the East China Sea during the summer of 2013, Cont. Shelf Res., 123, 99–110, doi:10.1016/j.csr.2016.05.001, 2016.

Wang, L., Zheng, B., Nan, B., and Hu, P.: Diversity of bacterial community and detection of *nirS*- and *nirK*-encoding denitrifying bacteria in sandy intertidal sediments along Laizhou Bay of Bohai Sea, China,

810   Mar. Pollut. Bull., 88(1–2), 215–223, doi:10.1016/j.marpolbul.2014.09.002, 2014.

Wei, W., Isobe, K., Nishizawa, T., Zhu, L., Shiratori, Y., Ohte, N., Koba, K., Otsuka, S. and Senoo, K.: Higher diversity and abundance of denitrifying microorganisms in environments than considered previously, ISME J. 9(9), 1954–1965, doi:10.1038/ismej.2015.9, 2015.

De Wilde, H. P. J. and De Bie, M. J. M.: Nitrous oxide in the Schelde estuary: Production by nitrification

815   and emission to the atmosphere, Mar. Chem., 69(3–4), 203–216, doi:10.1016/S0304-4203(99)00106-1, 2000.

Wittorf, L., Roger, F., Alsterberg, C., Gamfeldt, L., Hulth, S., Sundback, K., Jones, C. M. and Hallin, S.: Habitat diversity and type govern potential nitrogen loss by denitrification in coastal sediments and differences in ecosystem-level diversities of disparate N_2O reducing communities, FEMS Microbiol.

820   Ecol. 96(9), 1–9, doi:10.1093/femsec/fiaa091, 2020.

Wrage, N., Velthof, G. L., Van Beusichem, M. L., and Oenema, O.: Role of nitrifier denitrification in the production of nitrous oxide, Soil Biol. Biochem. 33(12–13), 1723–1732, doi:10.1016/S0038-0717(01)00096-7, 2001.

Wu, J., Chen, N., Hong, H., Lu, T., Wang, L., and Chen, Z.: Direct measurement of dissolved N_2 and denitrification along a subtropical river-estuary gradient, China. Mar. Pollut. Bull. 66(1–2), 125–134, doi:10.1016/j.marpolbul.2012.10.020, 2013.

Yamagishi, H., Westley, M. B., Popp, B. N., Toyoda, S., Yoshida, N., Watanabe, S., Koba, K. and Yamanaka, Y.: Role of nitrification and denitrification on the nitrous oxide cycle in the eastern tropical North Pacific and Gulf of California, J. Geophys. Res., 112, 1–15, doi:10.1029/2006JG000227, 2007.

Yan, W., Yang, L., Wang, F., Wang, J., and Ma, P.: Riverine N_2O concentrations, exports to estuary and emissions to atmosphere from the Changjiang River in response to increasing nitrogen loads, Global Biogeochem. Cycles, 26(4), doi:10.1029/2010GB003984, 2012a.

Yan, X. L., Zhai, W. D., Hong, H. S., Li, Y., Guo, W. D., and Huang, X.: Distribution, fluxes and decadal changes of nutrients in the Jiulong River Estuary, Southwest Taiwan Strait, Chinese Sci. Bull. 57(18), 2307–2318, doi:10.1007/s11434-012-5084-4, 2012b.

Yan, X., Wan, X. S., Liu, L., Xu, M. N., Tan, E., Zheng, Z., Zou, W., Tian, L., Li, D. W., Trull, T. W. and Kao, S. J.: Biogeochemical dynamics in a eutrophic tidal estuary revealed by isotopic compositions of multiple nitrogen species, Journal of Geophysical Research : Biogeosciences, 1849–1864, doi:10.1029/2018JG004959, 2019.

Yan, X. L., Zhai, W. D., Hong, H. S., Li, Y., Guo, W. D. and Huang, X.: Distribution, fluxes and decadal changes of nutrients in the Jiulong River Estuary, Southwest Taiwan Strait, Chinese Sci. Bull., 57(18), 2307–2318, doi:10.1007/s11434-012-5084-4, 2012b.

Yao, Y., Tian, H., Shi, H., Pan, S., Xu, R., Pan, N., and Canadell, J. G.: Increased global nitrous oxide emissions from streams and rivers in the Anthropocene, Nat. Clim. Chang., 10(2), 138–142, doi:10.1038/s41558-019-0665-8, 2020.

Yu, S., Yao, P., Liu, J., Zhao, B., Zhang, G., Zhao, M., Yu, Z. and Zhang, X. H.: Diversity, abundance, and niche differentiation of ammonia-oxidizing prokaryotes in mud deposits of the eastern China marginal seas, Front. Microbiol., 7(FEB), 1–13, doi:10.3389/fmicb.2016.00137, 2016.

Zhang, G. L., Zhang, J., Liu, S. M., Ren, J. L., and Zhao, Y. C.: Nitrous oxide in the Changjiang (Yangtze

850   River) Estuary and its adjacent marine area: Riverine input, sediment release and atmospheric fluxes,

Biogeosciences, 7(11), 3505–3516, doi:10.5194/bg-7-3505-2010, 2010.

Zhang, G., Zhang, J., Ren, J., Li, J., and Liu, S.: Distributions and sea-to-air fluxes of methane and nitrous

oxide in the North East China Sea in summer, Mar. Chem., 110(1–2), 42–55,

doi:10.1016/j.marchem.2008.02.005, 2008.

855   Zhang, J.: Biogeochemistry of Chinese estuarine and coastal waters: nutrients, trace metals and

biomarkers, J. Mater. Cycles Waste Manag., 3(1-3), 65–76, doi:10.1007/s10113-001-0039-3, 2002.

Zhang, Y., Xie, X., Jiao, N., Hsiao, S. S. Y., and Kao, S. J.: Diversity and distribution of *amoA*-type

nitrifying and *nirS*-type denitrifying microbial communities in the Yangtze River estuary,

Biogeosciences, 11(8), 2131–2145, doi:10.5194/bg-11-2131-2014, 2014.

860   Zhao, S., Wang, Q., Zhou, J., Yuan, D., and Zhu, G.: Linking abundance and community of microbial

N_2O-producers and N_2O-reducers with enzymatic N_2O production potential in a riparian zone, Sci. Total

Environ., 642, 1090–1099, doi:10.1016/J.SCITOTENV.2018.06.110, 2018.

Zheng, Z. Z., Wan, X., Xu, M. N., Hsiao, S. S. Y., Zhang, Y., Zheng, L. W., Wu, Y., Zou, W. and Kao,

S. J.: Effects of temperature and particles on nitrification in a eutrophic coastal bay in southern China, J.

865   Geophys. Res. Biogeosciences, 122(9), 2325–2337, doi:10.1002/2017JG003871, 2017.

Zhu, Z. Y., Zhang, J., Wu, Y., Zhang, Y. Y., Lin, J., and Liu, S. M.: Hypoxia off the Changjiang (Yangtze

River) Estuary: Oxygen depletion and organic matter decomposition, Mar. Chem., 125(1–4), 108–116,

doi:10.1016/j.marchem.2011.03.005, 2011.
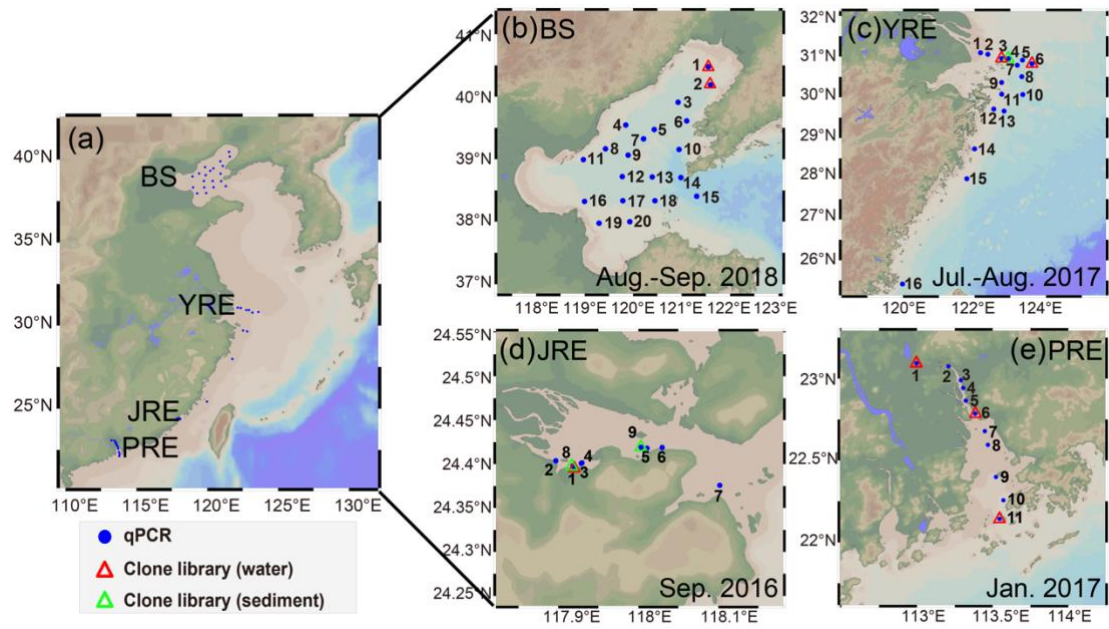
Figure 1. (a) Sampling sites in the four estuaries along China's coastline; **(b)** Bohai Sea (BS); **(c)** Yangtze River Estuary (YRE); **(d)** Jiulong River Estuary (JRE); **(e)** Pearl River Estuary (PRE). The sampling time for each region is shown in the subplots. The figure was produced by Ocean Data View 5.2.0 (http://odv.awi.de/).

870
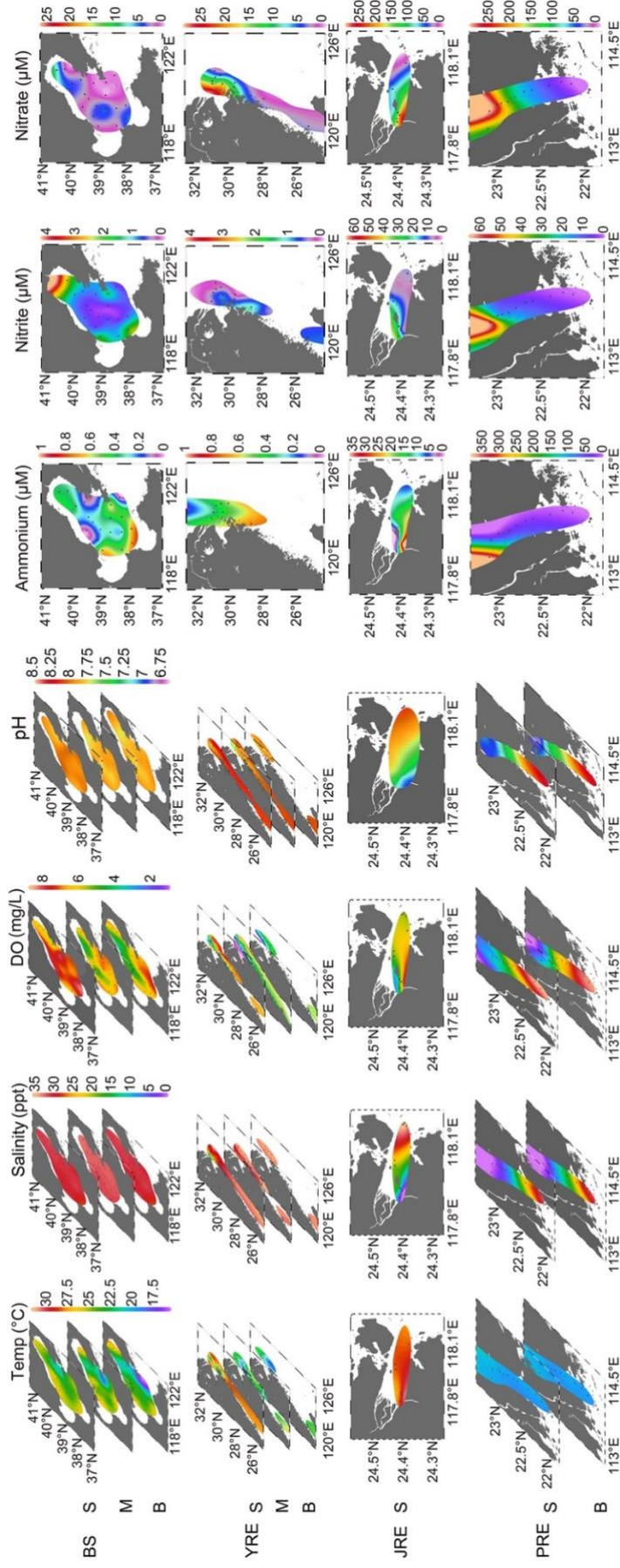
Figure 2. Temperature (Temp), salinity, dissolved oxygen (DO), pH, ammonium, nitrite, and nitrate concentration distributions in the Bohai Sea (BS), Yangtze River Estuary (YRE); Jiulong River Estuary (JRE); and Pearl River Estuary (PRE). Data from the surface layer (S), middle layer (M), and bottom layer (B) were shown for temperature, salinity, DO, and pH. Depth integrated mean values were used for ammonium, nitrite, and nitrate concentration distributions.
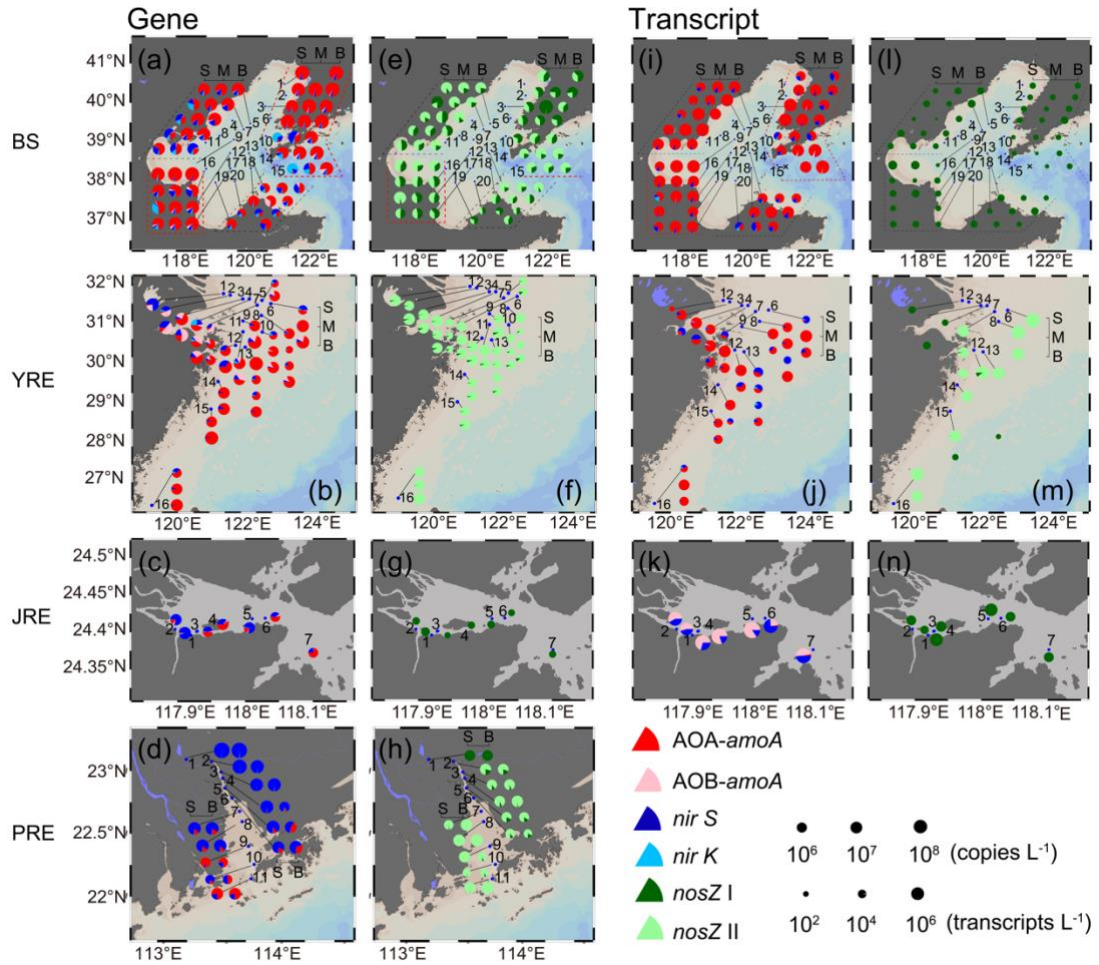
Figure 3. Six key functional gene and transcript abundance distributions in the Bohai Sea (BS), Yangtze River Estuary (YRE); Jiulong River Estuary (JRE); and Pearl River Estuary (PRE). S, surface layer; M, middle layer; B, bottom layer. **(a)**–**(d)** Gene related to N_2O production; **(e)**–**(h)** Gene related to N_2O consumption; **(i)**–**(k)** Transcript related to N_2O production; **(l)**–**(n)** Transcript related to N_2O consumption.
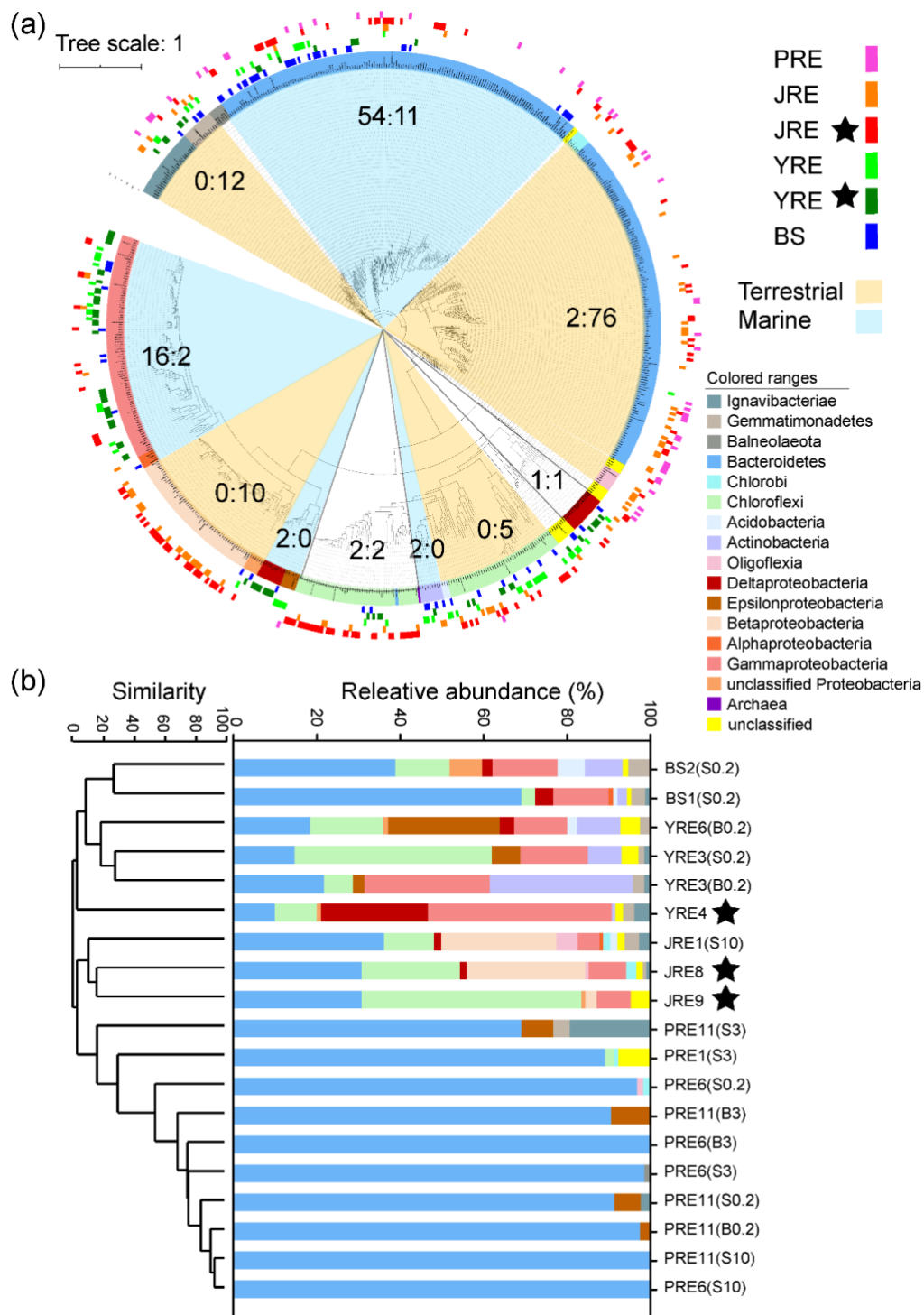
880

Figure 4. **(a)** Maximum likelihood phylogenetic tree of amino acid sequences of the clade II-type *nosZ*. The colors of the inner circle indicate taxonomic affiliations based on reference sequences. The colors of the outer circles represent the sources of clone sequences. The phylogenetic tree was bootstrapped 500 times. The scale bar represents the number of amino acid substitutions per site. Numbers before and after the colons indicate the number of reference

885 sequences from marine and terrestrial habitats, respectively. The figure was produced using the interactive tree of life (http://itol.embl.de/; Letunic and Bork 2016). **(b)** Relative abundances of community compositions of the clade II-type *nosZ* gene clone libraries in the four estuaries. The colors of the bars indicate taxonomic affiliations. The similarity was calculated from Bray–Curtis similarity. Black stars indicate sediment samples.
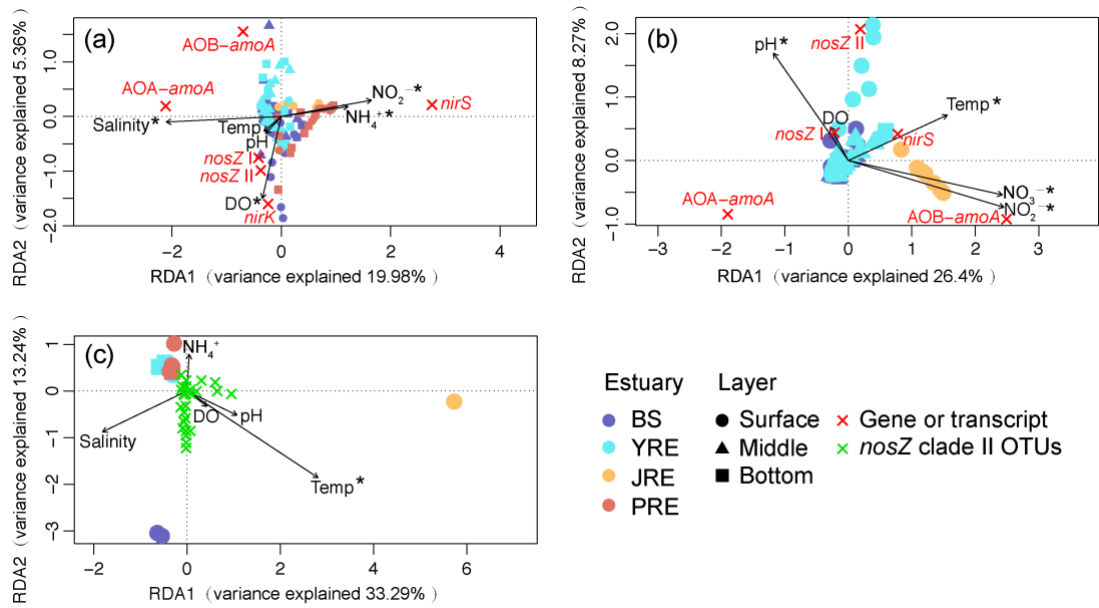
Figure 5. Redundancy analysis of the relative abundances of ammonia-oxidizing archaeal *amoA* (AOA-*amoA*), bacterial *amoA* (AOB-*amoA*), *nirS*, *nirK*, and *nosZ* clade I and II **(a)** genes and **(b)** transcripts, as well as of **(c)** the community composition of the *nosZ* clade II clone libraries under biogeochemical constraints. Each circle, triangle, or square represents an individual sample from the surface, middle, or bottom layer, respectively. The fork-shaped symbol represents the functional gene, transcript, or *nosZ* clade II OTU. Vectors represent environmental variables. Asterisks indicate statistically significant variables. Temp, temperature; DO, dissolved oxygen.
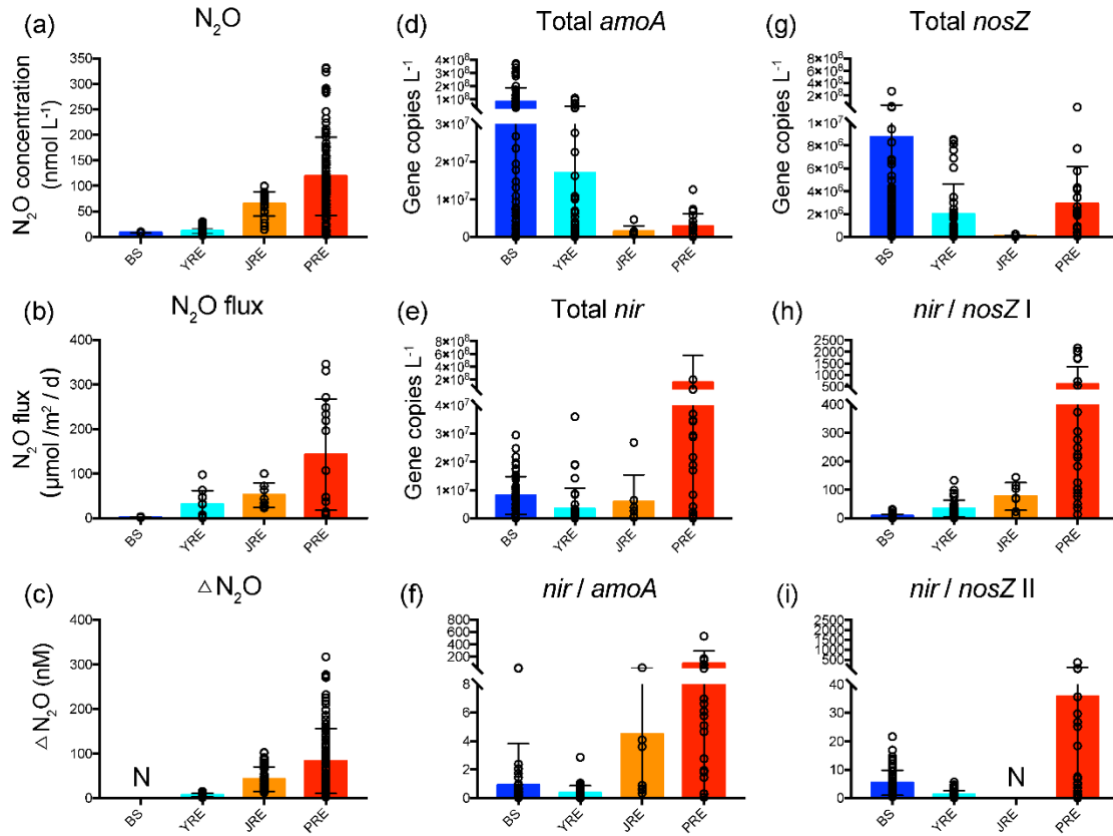
Figure 6. The ranges of **(a)** N₂O concentration, **(b)** N₂O flux, **(c)** ΔN₂O (data from Chen et al., 2008; Lin et al., 2016, 2020; Ma et al., 2019; Song et al., 2015; Wang et al., 2014, 2016; Wu et al., 2013; Xu et al., 2005; Zhan et al., 2011; Zhang et al., 2008, 2010), **(d)** total archaeal and bacterial *amoA* gene abundance, **(e)** total *nirS* and *nirK* gene abundance, **(f)** the ratio of total *nir* to *amoA* gene abundance, **(g)** total *nosZ* clade I and II gene abundance, **(h)** the ratio of total *nir* to *nosZ* clade I gene abundance, and **(i)** ratio of total *nir* to *nosZ* clade II gene abundance in the Bohai Sea (BS), Yangtze River estuary (YRE), Jiulong River estuary (JRE), and Pearl River estuary (PRE). Black circles represent the value of each sample. Bars represent the mean values. Error bars indicate standard deviation. N, no data or not determined.